

Modern sedimentation on the eastern continental shelf of India: Assessing the provenance and sediment dispersal pattern

Mascarenhas–Pereira, M.B.L.^{1*}, B. Nagender Nath^{1.}, Neetu, S^{1.}, Rifa Angela Rebelo^{2.}, Tyson Sebastian^{1,3.}, Sarkar, A^{4.}, Kazip, A^{5.}, Ajeesh, M.S^{5.}, Pavan Miriyala^{6.}, Patil, J^{1.}, Kocherla, M^{1.}, B. Ramalingeswara Rao^{7.}, Parthiban, G^{1.}

¹CSIR National Institute of Oceanography, Dona Paula, Goa, 403 004, India.

² 33 Albion Road, Hounslow Middlesex TW3 3RS.

³National Centre for Polar and Ocean Research, Ministry of Earth Sciences, Government of India, Headland Sada, Vasco-da-Gama, Goa 403 804, India.

⁴Regional Research Station (Red & Laterite Zone), Bidhan Chandra Krishi Viswavidyalaya, Paschim Medinipur, Jhargram, West Bengal, India.

⁵National Centre for Sustainable Coastal Management, Anna University campus, Chennai, 600025 India.

⁶CSIR-National Geophysical Research Institute, Hyderabad, India.

⁷CSIR-National Institute of Oceanography, Regional Center, Visakhapatnam, India.

*Corresponding Author: E-mail address: mariab@nio.org (M.B.L. Mascarenhas–Pereira)

Abstract

Sediments deposited on the eastern continental shelf of India are studied for texture, mineralogy and their major, trace, and rare earth elemental composition in lithogenic fraction. The objective of this study was to identify the sources, and evaluate the factors affecting the erosion and weathering in the catchment and dispersal and deposition of sediments over the shelf region. Here, we present an extensive dataset covering the entire eastern continental shelf of India from the Ganges-Brahmaputra (G-B) basin in the north including the shelf off major peninsular Indian river basins of Mahanadi, Godavari, and Krishna up to the Kaveri basin in the southern tip. Textural and geochemical studies have shown that the lithology of the source rocks plays an important role in governing the chemistry and mineralogy of the sediments. The results show that the G-B shelf sediments are primarily derived from the Higher Himalaya Crystalline sequence (HHCS) and the Tethyan sedimentary series (TSS) exposed along the peaks and drainage divide of the Himalayas. Mahanadi shelf sediments are mainly derived from the felsic rocks belonging to Precambrian metamorphic formations of the Eastern Ghats, limestones, sandstones, and shales of the Gondwanas and recent deltaic alluvium deposits, whereas the Krishna-Godavari (K-G) sediments find a part of their source in the Deccan Basalts. The shelf sediments off River Kaveri are derived from a mixture of peninsular granitic gneisses, tonalite-trondjhemite gneisses, and charnockites. The sediment geochemistry has also allowed us in assessing the weathering patterns in the source areas. The sediments have undergone a moderate degree of weathering. Weathering intensities were found to have varied with the source area lithology.

The least square regression of the geochemical data allowed us to estimate the relative contribution of each of these sources and their geographic extent. Unlike the massive offshore deposition and formation of a major Fan system (the Bengal fan), the fluvial sediment dispersal of the mighty Himalayan Rivers on the continental shelf is significant only at the G-B mouth and their contribution reduces to <50% at about 18°N. The sediment dispersal from the Godavari River is seen to extend on either side of the mouth of the river which is attributed to the reversing East India Coastal Current (EICC), which plays an important role, in the sediment transport along the central and south-central part of the east coast of India. The influence of the Mahanadi, Krishna, and Kaveri River sediments is however confined to a small area near their mouths and has a limited geographic extent of influence in the shelf region.

Key words : Eastern continental margin of India, sediment dispersal, provenance, clay mineralogy, geochemistry

1. Introduction

The continental shelf is a continuum of the continent connecting the deep sea, and thus a key interface between the land and sea and a depocenter of terrigenous sediments. The sediments deposited on the continental shelf regions record environmental and climatic information (France-Lanord and Derry, 1997; Galy et al., 2007; Liu et al., 2016) and in recent years, the shelf studies have attracted various international research projects (e.g., MARGINS, LOICZ). The eastern continental shelf of India is one of the world's most extensive continental shelves, which is surrounded by rivers of different scales that input a huge amount of terrigenous sediment into the Bay of Bengal, and acts as a conduit for sediment spreading to large, distant areas with formation of submarine Bengal fan (Curry et al., 2002) and subaqueous river deltas such as Krishna, Kaveri and Godavari (Loucks et al., 2019). This enormous riverine sediment delivery has a strong bearing on many important global and oceanographic processes, affecting ocean productivity and biogeochemistry. Mighty Himalayan rivers G-B constitute the two most important sources of terrigenous sediments in the Bay of Bengal. Nevertheless, the contribution of small and medium-sized peninsular Indian rivers along the east coast also needs to be considered (Milliman, 2001). The G-B rivers in combination with the peninsular Indian rivers (Godavari, Krishna, and Mahanadi supply about 1350 million tons of fluvial sediment loads annually and contribute about 8% of the global river supply to the ocean (Milliman, 2001) and thus significantly influence the global sediment cycling and marine ecosystems.

Seasonally reversing surface circulation controlled by the monsoon (Shankar et al., 2002) and the local coastal currents influence the dispersion and deposition of these sediments. A quantitative assessment of the dispersal pattern of fluvial-derived sediments is necessary to decipher the future fate of the densely populated mega-deltas that depend largely on their overall sediment budget (Syvitski et al., 2009). Furthermore, the shallow continental shelf areas are increasingly used for various developmental purposes (e.g., transportation, aquaculture, mining, fishery, and tourism) which can affect the seabed sediment composition and accumulation pattern and also can introduce pollutants.

The primary objectives of this study are to decipher the spatial variation in the dispersion of lithogenic sediments in the eastern continental shelf of India (ECSI), to identify their source and relative contribution of competing sources to the sediments in the area, and to assess the transport pathways along the shelf using inorganic geochemical tracers. For this, 65 surface sediments from the entire ECSI were studied. While the entire shelf from north (off Bengal) to south (off Tamil Nadu) was covered, an emphasis was given to sampling the shelf in the vicinity of all major and

minor river mouths (Fig. 1). This study provided an opportunity to study the geochemical nature of sediments deposited at river mouths, to trace the natural dispersal pattern in the shelf and to delineate the extent of influence of each source identified. Using geochemical discrimination criteria, the role of climate and local geology in controlling the erosion and weathering patterns in the catchment areas was assessed.

While the earlier studies have either focused on smaller areas on ECSI shelf (e.g., Subba Rao, 1964; Subramanian et al., 1985; Seralathan and Seetharamaswamy, 1987; Subramanian and Mohanachandran, 1990; Paropkari, 1990; Veerasingam et al., 2014; Tripathy et al., 2014; Bejugam and Nayak, 2016; Symphonia and Nathan, 2018; Pattan et al., 2008; Majumdar et al., 2014), or broad basin-wide distribution pattern (e.g., Wijayananda and Cronan, 1994; Roonwal et al., 1997; Li et al., 2017; Mohanty et al., 2008; Sebastian et al., 2019), this forms the first comprehensive report of geochemical characterization of entire ECSI. The western continental margin has been extensively studied for geochemistry (see Kurian et al., 2013 and references therein), whereas, although the eastern continental margin acts as a depocenter for many rivers, no study has been carried out covering the entire shelf. In addition to defining the regional trends of elemental variation, an attempt is made to employ an inverse model technique to quantify the relative contribution of each of the sources identified.

1.1. Physiographic setting and oceanography of the study area

The east coast of India has a length of 2686 km. The ECSI covers an area of about 0.13×10^6 km² and its width is maximum off the Ganges (210 km) and a minimum off Karaikal in Tamil Nadu (16 km). It is aligned in a NE-SW trend. The Eastern coastal plain (ECP) which separates the Eastern Ghats from the Bay of Bengal and varies between 100 and 130 km in width (Fig. 1). The rivers on the East coast have a number of large and small estuaries which ultimately form deltas.

The northern Indian Ocean is characterized by seasonally reversing surface circulation controlled by the reversal in the wind direction caused by the monsoon (Shankar et al., 2002) and may influence the dispersion and deposition of suspended sediments significantly. A northeast-flowing current associated with the southwest monsoon winds (May-September), a southwest-flowing current associated with the northeast monsoon winds (November-February), and waves that rarely exceed 3 meters in height are the chief distributive agents of this sedimentary reflux onto the shelf. In storms of exceptional intensity, waves as high as 12 meters are expected to occur in the Bay (Dube et al., 1997) and can churn up the bottom sediments and cause their redistribution. The East India coastal current (EICC) is the major surface current that affects the coastal hydrodynamics

around India (Shankar et al., 2002). Longshore sediment transport direction in this area is highly variable. While the drift is bi-directional and varies with season, the net transport is northwards (e.g., Kumar et al., 2006).

Geology of the Eastern Continental margin and the adjoining river basins

The east coast of India has evolved through multiple phases of tectonic activity and is fed by an abundant supply of sediments brought by prominent river systems of the Indian Shield. The sediments of the Eastern Continental Margin of India (ECMI) are mainly derived from Himalayan and Peninsular Indian river sources. The G-B River system carries the sediments derived from the weathering of the Himalayas, while the rivers Mahanadi, Krishna, Godavari, Palar, and Kaveri (Fig 1) drain peninsular India. The G-B River system is the predominant source of sediment input to the Bay of Bengal and the enormous sediment influx resulted in the formation of the Bengal Fan (e.g., Curray et al., 1983), which is the world's largest sediment depocenter (eg. Alam et al., 2003). The southern extent of Fan sedimentation and the turbiditic sedimentation from G-B rivers reach the south of the equator until the northern part of the Central Indian Basin (Nath et al., 1989). The principal source rocks for the G-B sediments include the Higher Himalayan crystalline series (HHCS) (e.g., Nath et al., 2005), Lesser Himalayas (LH), Trans-Himalayan batholiths (THB), and Tethyan Sedimentary series (TSS) (e.g., Singh et al., 2008). Along with the G-B sediments, fluvial sediments received from the southern rivers like Mahanadi, Krishna- Godavari (K-G), Palar, and Kaveri also contribute to the shelf sediment load.

Mahanadi Basin extends from Jagannathpur in the north to Chilka Lake in the south and further extends offshore into the Bay of Bengal (Fig. 1). The Mahanadi River basin is characterized by a tropical climate. Late Archaean and early Proterozoic granite batholiths, tonalite-trondjemite gneisses (TTGs), charnockites and khondalites of the Eastern Ghats constitute the major part of the catchment area. Sedimentary rocks such as limestone, shale, and sandstone and recent alluvium/littoral deposits constitute the remaining part of the drainage area (e.g., Chakrapani and Subramanian, 1990). The geologic history of the K-G Basin is similar to that of the Mahanadi Basin. The K-G basin extends offshore along the ECMI. The K-G rivers open to the Bay of Bengal in the southern state of Andhra Pradesh. The Godavari River flows through the states of Maharashtra, Telangana, Andhra Pradesh, Chhattisgarh, and Odisha in addition to smaller parts in Madhya Pradesh, Karnataka, and the Union territory of Puducherry, while the Krishna River flows through Maharashtra, Karnataka, and Andhra Pradesh (Fig. 1). The source rocks for Godavari sediments are Deccan trap basalts, late Archaean/early Proterozoic granites, Precambrian and Gondwana sedimentary rocks and recent alluvial cover (Rengasamy et al., 2005). The major geological

formations in the drainage basin of Krishna River include major rock types of Archaean and Younger crystalline rocks (78%), with considerable contribution from the Tertiary Deccan Traps (20%) and recent alluvial (2%) cover (Ramesh et al., 1989) (Table 1).

The Kaveri basin is located in the southeastern part of Peninsular India. Archaean metamorphic and igneous rocks with a well-marked NE-SW Eastern Ghat trend constitute the basement. The basin, for the most part, is covered by Holocene deposits. Archaean granites and gneisses are found to the northern and western limits and extend offshore towards the east. The Kaveri River drains through the metamorphic (Peninsular granite gneiss, charnockite, etc.) and igneous (Closepet granite) terrains belonging to the Precambrian formations of South India i.e. Dharwar system (Vaithyanathan et al., 1992).

2. Materials and Methods

2.1. Coring and sub-sampling

The surface sediments were collected using a box corer from the ECSI on board the research vessel Sindhu Sankalp during her cruises SSK-35 and 50 during the 'Source to Sink' studies of project GEOSINKS. Sediments were collected from the uppermost layer of the core taking care to minimize the mixing with subsurface sediments to represent the modern sedimentation. Sampling locations are shown in Figure 1 and the details of core locations are given in Table 2.

2.2. Textural and clay mineralogical analysis

Textural analysis was carried out using a combination of wet sieving and pipette analyses method. Sediment samples were desalinated by washing repeatedly with deionized water and dried at 45°C. Samples of 13 g were disaggregated in deionized water and passed through a 63- μm sieve to separate the sand from the mud fraction. The < 63 μm fraction was thoroughly homogenized into a suspension and analyzed for grain size using a Laser Diffraction Particle Size Analyzer (Malvern Mastersizer 2000). Prior to analysis, sediment samples were decarbonated using dilute HCl (1N) and 10% H₂O₂ to remove organic carbon, which was then ultrasonicated before analysis.

For clay mineralogy, the clay fraction (< 2 μm sediment fraction) was separated from the sediments using Stokes settling velocity principle. This clay fraction was deposited on glass slides. Oriented slides were prepared by pipetting 1 ml of clay suspension. These slides were air-dried and treated with ethylene glycol at 100°C for 1 h. Subsequently, these clay deposited slides were scanned from 3° to 30° 2 θ on a Rigaku X-ray diffractometer using nickel-filtered Cu Ka radiation. Clay minerals were identified following Biscaye (1965) and quantified as relative percentages.

2.3. Geochemical analyses

Major oxide analyses were carried out on a salt-free lithogenic fraction of sediments using a PANalytical X-ray Fluorescence Spectroscopy (XRF) Model Axios. Ten grams of sediment were made salt-free with repeated washings with distilled water, which was followed by calcium carbonate removal by repeatedly adding 20% acetic acid until the effervescence ceased. The decarbonated sediments were dried and powdered. An aliquot of the decarbonated sample was dried in a hot air oven at 110°C for at least 12 hours. This moisture-free sample (~ 0.55g) was mixed with 5.5 g of fusion mixture (A-100 Di-Lithium Tetra Borate with 0.07% Lithium Bromide) at a ratio of 1:10, homogenized, converted to melt at 1100°C in a platinum crucible (MiniFuse2) and allowed to cool to become a glass bead. The accuracy of the data was assessed using the international standard reference material (JMS-1) and found to be better than $\pm 5\%$ for all the elements

Fifty milligrams of salt-free sediment sample was dissolved in 10 ml of an acid mixture (HF, HNO₃, and HClO₄) in a proportion of 7:3:1 in a PTFE beaker by heating on a hotplate. For HF and HNO₃ supra pure grade (MERCK) acids were used. An additional 5 ml of acid mixture was added for complete dissolution. The semi-dry solution was redissolved in 4 ml of 1:1 suprapure HNO₃ and subsequently diluted to 100 ml using ultrapure distilled water. International reference materials (MAG-1 Marine Sediment) and SCo-1 (Cody Shale) of the United States Geological Survey were digested following the above protocol used for samples. These solutions were analyzed for trace and rare earth elements (REEs) using an Inductively Coupled Plasma Mass Spectrometer (ICP-MS Thermo X series-2). The accuracy of the data was better than $\pm 8\%$.

3. Results

3.1. Texture

Textural data are presented in Table 3 and the regional distribution maps of sand, silt and clay content are shown in Fig. 2. Sand content is variable with the highest content in Kaveri shelf sediments (avg. 63 wt%), followed by Mahanadi (avg. 40 wt%) and G-B (avg. 20.4 wt%) while the K-G shelf sediments has lower sand content (avg. 2.8 wt%). The sand content gradually decreases away from the coast. The average sand content is ~ 40%. Silt content is variable with some having high content (61%). The high silt content (upto 61%) is observed along the shelf off G-B, Mahanadi and K-G while Kaveri shelf sediments show low content (< 30%). The clay content ranges from <1% (Kaveri shelf sediments) to 75% (K-G shelf sediments). The average clay content is highest at the mouth of the Krishna River (54 %) while G-B and Mahanadi shelf sediments shows moderate content above 20%.

3.2. Clay minerals

Smectite content in the G-B, Mahanadi, K-G and Kaveri shelf sediments (Table 3, Fig. 3) range from 37 to 91% (avg. 55%), 37 to 69% (avg. 52%), 55 to 97% (avg. 76%) and 41 to 100% (avg. 74%), respectively. The smectite content in southern part (south of 18° N) of the continental shelf is high (avg. 74%) as compared to the northern part (north of 18° N) (avg. 52%). The distribution of illite and smectite content along the ECSI show a mirror image pattern of distribution. The northern shelf sediments (north of 18°) is enriched in illite which may be contributed by rivers G-B (avg. 25%) and Mahanadi (avg. 17%). Mahanadi shelf sediments are enriched in kaolinite (avg. 28.5%) compared to G-B shelf sediments which exhibits low content (avg. < 15%). G-B shelf sediments are abundant with chlorite (upto 15%), while Mahanadi and K-G shelf sediments have similar contents (avg. 2%) of chlorite with high contents away from the shelf. Kaveri shelf sediments exhibit average chlorite content of 1.3%.

3.3. Geochemical data

The geochemical data of the sediments along the ECSI studied here are presented in Tables 4 and 5. Regional distribution maps of major elements and total REEs are presented in Figs. 4 and 5. The SiO₂ (wt%) ranges from 43 to 88% (avg. 63%). The G-B, Mahanadi and Kaveri shelf sediments have higher SiO₂ content (avg. >62 wt%) compared to the K-G shelf sediments (avg. 56 wt%). The Al₂O₃ (wt%) concentration range from 3.08 to 22% (avg. 15%). The Fe₂O₃ (wt%) content ranges from 2.71 to 13.24% (avg. 8.03%), except for a sample along the Kaveri shelf (max. 22%). The K-G shelf sediments have highest Fe₂O₃ content (avg. 11.17 wt%) compared to other shelf sediments such as the G-B (avg. 6.71 wt%), Mahanadi (avg. 8.09 wt%) and Kaveri (avg. 7.94 wt%) shelf sediments (Table 5; Fig 4). TiO₂ (wt%) content ranges from 0.61 to 4.16 wt% (avg. 1.16%), with K-G shelf sediments containing higher content (avg. 2.31%) compared to G-B (avg. 0.84%), Mahanadi (avg. 1.29%) and Kaveri (avg. 0.93%) shelf sediments. MgO content also exhibits a similar distribution like TiO₂, with higher content in K-G shelf sediments (avg. 2.59%) compared to G-B (avg. 2.27%), Mahanadi (avg. 1.63%) and Kaveri (avg. 2.09%) shelf sediments. CaO (wt%) ranges from 0.42 to 8.7wt % (avg. 1.59%), while Na₂O content (wt %) ranges from 0.34 to 2.95 (avg. 0.92%). The K₂O concentration (wt%) in the sediments of the ECSI range from 0.75 to 4.05% (avg. 2.34%).

The total REEs concentration varies from 69 to 891ppm (Table 5; Fig. 5). The total REEs concentration in the G-B, Mahanadi, K-G and Kaveri shelf sediments vary from 136 to 305ppm (avg. 207ppm), 119 to 892ppm (avg. 284 ppm), 140 to 215ppm (avg. 181 ppm) and 65 to 497ppm (avg. 180ppm) respectively. REE values are normalized with Post Archaean Australian Shale (PAAS)

values (Taylor and McLennan, 1985). The PAAS normalized REE distribution patterns of the G-B, Mahanadi, K-G and Kaveri shelf sediments are presented in Figure 6. Most of the shale-normalized REEs have sample/PAAS ratio close to 1 (Fig. 6). The sediments show REE patterns enriched in LREE compared to the HREE throughout the eastern continental shelf except for the K-G shelf sediments and one sample from Kaveri (SPC 46) shelf. LREE are enriched in the G-B shelf sediments while depleted in the southern stations (K-G and Kaveri shelf sediments) (Fig. 6). Cerium (Ce) and Europium (Eu) anomalies and fractionation indices are calculated following Nath et al. (1997 and references therein). Compared to their lanthanide neighbors which occur only in trivalent oxidation state, Ce and Eu can occur in response to change in oxidation state, resulting either in positive or a negative departure from their trivalent neighbors. Eu anomaly in sediments is mainly inherited from their parent material and thus can be diagnostic of source material. The Ce and Eu anomaly ranges from 0.93 to 1.28 and 0.24 to 1.98 respectively. The Eu and Ce anomaly in the G-B shelf sediments are 0.9-1.21 (avg. 1.03) and 0.99-1.28 (avg. 1.1) respectively, Mahanadi shelf sediments have Eu and Ce anomaly in the range of 0.24 to 1.1 (avg. 0.94) and 1.01 to 1.25 (avg. 1.14) respectively, K-G shelf sediments have Eu and Ce anomaly in the range of 1.16 to 1.51 (avg. 1.33) and 1.06 to 1.22 (avg. 1.1) respectively, while Kaveri shelf sediments they vary from 0.49 to 1.98 (avg. 1.29) and 0.93 to 1.24 (avg. 1.1) respectively. The average $(La/Yb)_n$ ratios for the G-B shelf sediments is 1.5, Mahanadi shelf sediments is 1.36, K-G shelf sediments is 0.82 and Kaveri shelf sediments is 1.31.

4. Discussion

4.1. Textural control on chemistry

Once the sediments are deposited at the river mouth along the coast, fluvial processes of transportation, sorting, and deposition affect the chemical characteristics of clastic sediments. Sediments are carried and deposited under different fluvial regimes at different sites. The hydrological differentiation processes that operate on the coastal sediments such as hydrodynamics, sorting, and bottom currents can fractionate the coarser from finer sediments depending on the energy conditions of the stream and can define the sediment chemistry. The surface sediments along the ECSI exhibit a wide range of sand and silt content. Overall the shallower depths are sandy compared to the deeper depths which have high clay content. No textural control is seen for the refractory element Ti in these sediments. A plot of TiO_2 versus sand, silt, and clay content (Fig. 7a, b, c) shows no discernible trend with texture but varies distinctly for each area with the highest values for all K-G and Mahanadi shelf sediments. Thus Ti, as perceived before (e.g., Kurian et al., 2013) is a robust indicator of provenance and is less affected by textural sorting in this area. On the other

hand for aluminum, another diagnostic indicator of source, a negative relation between Al_2O_3 and sand is seen (Fig. 7d) but a fairly positive relation with the finer fractions of silt (Fig. 7e) and clay content (better relation than with silt) (Fig. 7f) indicates that it is mostly contained in clay minerals.

Major alkaline and alkaline earth elements can be diagnostic of provenance. A plot of $\text{SiO}_2/\text{Al}_2\text{O}_3$ versus $\text{Na}_2\text{O}/\text{K}_2\text{O}$ (Fig. 7g) show a variation of $\text{Na}_2\text{O}/\text{K}_2\text{O}$ for each river sediment suite (with a minor overlap) despite the variation in sediment texture.. Previous studies on the mainstream Ganges River have shown high content of Na_2O , K_2O , and CaO (Singh, 2009) with sand + silt sediment fraction consisting mostly of quartz and feldspars. The G-B and Mahanadi shelf sediments exhibit high SiO_2 content but with low clay content (Fig. 2) indicating their mature nature. However, this relationship is not seen in the K-G and Kaveri shelf sediments. Among the three southern rivers (K-G and Kaveri), though the sand content in the Kaveri shelf sediments is variable, the sediment maturity of the three rivers is comparatively the same. The K-G shelf sediments however have a minimal amount of sand (avg. 8%) followed by silt (avg. 44%) and high content of clay (avg. 54%) (Table 3). The clay content is highest at the mouth of the Krishna River (> 50%), while G-B and Mahanadi shelf sediments show moderate content (> 30%). Low clay content seen along the coast of Orissa (Mahanadi shelf sediments) and Tamil Nadu (Kaveri shelf sediments avg. 20%) (Fig. 2) indicates deposition close to the source and poor transportation. The sediments of the northern two rivers (G-B and Mahanadi) however show higher sand content (20 and 40% respectively) with decreasing $\text{Al}_2\text{O}_3/\text{SiO}_2$ ratio (Fig. 7d), a ratio which is suggested to be a geochemical proxy for grain size (e.g., Galy et al., 2008). A plot of $\text{Al}_2\text{O}_3/\text{SiO}_2$ versus sand, silt, and clay shows an inverse trend with sand content and a fairly positive relation with silt and clay content (Fig. 7d, e, f) and supports the use of this ratio as an indicator of texture. A similar relationship is also observed in the case of REEs. In all samples studied, the coarser sediment fractions as inferred from $\text{Al}_2\text{O}_3/\text{SiO}_2$ ratio have higher REE abundance (Fig. 7h).

Interestingly, this is not the case with K-G shelf sediments where the REEs are hosted in the clay fraction. Our observation of REEs in different river shelf sediment domains i.e., G-B, Mahanadi, and Kaveri, and the inferred textural control suggest that fluvial processes of sorting is a secondary process and does not affect REE distribution in most of these river sediments. Therefore, we infer that a very large part of REE in these rivers seems to be present in the silicate minerals and associated phases in the G-B, Mahanadi, and Kaveri sediments. The K-G sediments on the other hand show a reverse trend, with a direct relation of $\text{Al}_2\text{O}_3/\text{SiO}_2$ ratio and REE abundance (see for similar observations by McLennan, 1989; Morey and Setterholm, 1997; Vital and Statterger, 2000).

This distribution is likely affected by the differential concentrations of various REE-holding minerals such as garnet, monazite, zircon, apatite, etc, and diluting minerals in different size fractions.

4.2. Major element geochemistry as provenance indicators

There is a progressive decrease in K_2O (Fig. 4) from G-B shelf sediments to the Kaveri shelf sediments suggesting a change in the lithology of the source rocks. Higher K_2O content (avg. 3.26%) in the G-B shelf sediments is attributed to a felsic source, which is related to a greater illite content (avg. 24.5%). The high content of K_2O in the G-B shelf sediments is probably due to the presence of feldspars like orthoclase and micas like muscovite and biotite. This is also supported by the high content of illite (Fig. 3) in the G-B shelf sediments. Siddiquie (1967) suggested that illite, kaolinite, and montmorillonite are the major clay minerals associated with the Himalayas and the rivers draining them. Higher K_2O , off Puri in Orissa (Fig. 4), maybe due to local geology of the Mahanadi drainage area. Mahanadi River drains mostly the amphibolites, and schist containing potassic feldspars which may be responsible for the high K_2O content. The Godavari shelf sediments are depleted in K_2O content (Fig. 4), indicating low illite and other K-micas in Godavari river sediments.

The Al_2O_3 concentrations are high i.e. 14-20% (Fig. 4) off Puri in Orissa, which may be due to the local geology of the area which is composed of granites containing high plagioclase content. The river Mahanadi flows through the state of Orissa and drains the felsic rocks of Precambrian metasediments, amphibolites and schists intruded by granite gneisses (Sastry et al., 1981). Amphibolites are usually composed of amphibole and plagioclase feldspars and may contain little or no quartz. High Al_2O_3 content corroborates well with the high kaolinite content (Fig. 3) in the area.

The K-G shelf sediments have high total iron (Fe) content converted from oxide data given in Table 4 (avg. 7.81 wt%) compared to the G-B (avg. 4.69 wt%), Mahanadi (avg. 5.64 wt%) and Kaveri (avg. 5.55 wt%) shelf sediments and much higher than the global average for continental margins (3.69 wt% see Poulton and Raiswell, 2002). The high Fe content (7.58 to 8 wt%) in the K-G shelf sediments may be attributed to iron-rich mafic source rock such as Deccan basalts in the catchment area (~9.1 to 11.2 wt% - see Peng et al., 1998; Bose, 1972). High Fe values are consistent with high magnetic susceptibility values in the K-G shelf sediments (Sebastian et al., 2019) which were attributed to their Deccan Basalt source. The G-B shelf sediments show relatively lower Fe values (4.69 wt%), but are similar to the average global river sediments (4.8 wt%) and also are closer to that in HHCS metasediments (4.6 wt%; Ayres and Harris 1997). There are other Fe-rich sources too in the Himalayan region (Ahmad et al., 1998) that can contribute to the G-B shelf.

Ti is another important diagnostic element for studying provenance (e.g., Kurian et al., 2013). The TiO₂ concentration is the highest in the K-G shelf sediments (max. 4.16 %) and lowest in the G-B shelf sediments (max 0.92%) compared to the other sediments along the ECSI (Fig. 4). Krishna River which flows through Maharashtra in the upper reaches and drains Deccan trap basalts containing calcic plagioclase and clinopyroxene with high Ti content. The unique character of Deccan traps is the presence of Ti-rich basalt (Brown et al., 2011). Weathering of minerals such as ilmenite, sphene/titanite would have contributed to high Ti content. Slight enrichment of TiO₂ is also seen in Godavari shelf sediments; the source again would be Deccan traps whereas rivers G-B sediments have a very low concentration of TiO₂, as G-B rivers drain through felsic rocks with low TiO₂ content (<1 wt%, Ayres and Harris, 1997; Ahmad et al., 1998). TiO₂ content (up to 4.16%) is also high off Puri in Orissa probably due to the presence of ilmenite.

In the A–CN–K (Al, Ca, Na, and K) diagram (Fig. 8), the shelf sediments from the Ganges, Mahanadi, K-G, and Kaveri are plotted. Also plotted are the values of potential source rocks which occur in the respective drainage basins. The sediment from a given river system (Fig. 9) which is closest to the coast is taken as representing the source of sediments to the deeper areas. A clear demarcation is seen in the compositional fields of all 4 regions. The clustering of all the shelf sediments from the north and south along an A-CN trend line indicates the different composition of their sources, with the northern shelf sediments (G-B and Mahanadi rivers) plot slightly away from the A-CN line and closer to the trend line joining PAAS, granites and a suite of lithologies comprising the HHCS and LH rocks. Interestingly the source sediments of Mahanadi and G-B plot close together and seem to have a common source rock. The progressive shift upwards on the A-CN trend line away from the source rocks is probably due to the addition of fine-grained mica group of minerals, which were removed as suspended load and were later incorporated into the sediments at the time of flooding (Chakrapani, 2005). Whereas the data for southern shelf sediments (K-G and Kaveri rivers) plot closer to the A-CN trend line with compositional similarity to basalts, charnockites, granites, gneisses, and PAAS. The upper reaches of the Kaveri River basin are lithologically dominated by a suite of gneisses, granites and charnockites. The gneisses found in the Kaveri drainage basin vary in composition from dioritic to granitic. The source sediments for the Kaveri shelf sediments plot between the mixing line of gneisses and basalt and thus have contributions from both felsic and mafic source s.

4.3. Trace elements as indicators of provenance

Trace elements such as Th, Sc, La, Co, and REEs have been used extensively in assessing the provenance of sediments (Nath et al., 2000 and references therein) as they are least affected by

secondary processes. These elements tend to be almost quantitatively transferred into the sediments. The elemental ratios of these elements such as Th/Sc, Th/Co, and La/Sc are also distinctly different for felsic and basic sources as the ratios include both compatible and incompatible elements (McLennan et al., 1990). Felsic rocks are richer in Th and La while Cr, Sc, and Co are enriched in basic rocks and thus these ratios are low for basic rocks.

A clear provinciality is seen in the Th/Sc ratios from north to south of the study area. The Th/Sc ratio for the G-B, Mahanadi, K-G, and Kaveri sediments ranges from 1.1 to 2.1 (avg. 1.38), 0.9 to 5.6 (avg. 1.84), 0.4 to 0.6 (avg. 0.51) and 0.8 to 9.5 (avg. 1.74) respectively (Table 4 and 5, Fig. 10a). A low Th/Sc ratio (<1) indicates a mafic source as the mafic rocks are usually enriched in compatible elements such as Sc, while the felsic rocks contain a higher concentration of Th, an incompatible element (McLennan et al., 1990). Typically for upper continental crust (UCC) and PAAS, the Th/Sc ratio is ~1 but higher for granitic rocks (3.75 to 10 - see Condie, 1993 for example).

The discrimination plot of Cr/Th versus Th/Sc (Fig. 10b) and TiO₂ (%) versus Ni (ppm) (Fig. 10c) are also used to constrain the sources to the ECSI sediments. While the mafic sources have high Cr/Th ratios, higher Th/Sc ratios are indicative of presence of felsic component. The sediments from the ECSI fit in a mixing hyperbolic curve between felsic and mafic end members (Fig. 10b). While the G-B sediments seem to be derived from a felsic source probably from the HHCS metasediments, Mahanadi and Kaveri shelf sediments fall along the mixing line joining the mafic and felsic sources indicating a mixed source of the mafic basaltic and felsic peninsular granitic and gneissic complex. The K-G shelf sediments however have higher values of Cr/Th ratio and plot closer to the mafic end member as they would probably receive a greater proportion of sediments from the Deccan Traps compared to other river sediments. The sediment source was further constrained using discrimination plot of TiO₂ versus Ni, which also separate immature sediments derived from magmatic precursors from normal mature sediments (Floyd et al., 1989). Figure 10c shows that most of the G-B, Mahanadi and Kaveri shelf sediments with low Ni and Ti abundances plot in fields typical of acidic and intermediate rocks, whereas the K-G shelf sediments with high TiO₂ and Ni contents plot in field typical of basic rocks.

Similarly, Co/Th ratio is used as a provenance indicator. Co is a compatible element, abundant in mafic minerals, while Th is an incompatible element abundant in felsic minerals (Cullers et al., 1988) and thus can be indicative of provenance composition (Taylor and McLennan, 1985). The average Co/Th ratio in the ECSI sediments (Fig. 10d) is the highest for the K-G shelf sediments (2.79), compared to Kaveri shelf sediments (1.49), Mahanadi (1.01), and G-B (0.86) shelf sediments.

Thus the Co/Th ratio too supports the interpretation of greater mafic contribution to the K-G shelf sediments and the least to the G-B sediments. In the discrimination plot of La/Sc versus Co/Th (Fig. 10d) too, K-G shelf sediments fall in a distinct group closer to basalt field with lower La/Sc ratios.

In the discrimination plot of La–Th–Sc (Fig. 11) the sediments cluster around UCC and are derived from the mixing of three end members i.e. granite-granodiorite-basaltic rocks. Like other elemental concentrations, ratios and discrimination plots, mafic contribution to the K-G shelf, with the K-G shelf sediments clustering together and plot relatively closer to the basalt end member as compared to the shelf sediments of the northern areas. The G-B shelf sediments plot along the granite-granodiorite mixing line and indicate their contribution to the sediments, while the sediments of Mahanadi and Kaveri shelves show a much wider distribution which probably indicates a mixed contribution from all three end members.

While the Th/U ratios in sedimentary rocks are in the range of 0.02 to 21 (Adams and Weaver, 1958), most marine sediments have ratios much <7. The high Th/U ratio of the G-B shelf sediments (Fig. 5; 5.5 to 9.3) may be due to monazites from the Monzonitic THB that are present in exposed outcrops of the Brahmaputra watershed (Goodbred et al., 2014). The Th/U ratio of the Mahanadi shelf sediments (2.2-29, except for one sample with a ratio of 33) falls along the mixing curve defined by the peninsular granitic and gneissic complex and the U-rich mineral deposits (of Proterozoic and Gondwana age) and monazites. The peninsular granite and gneisses have relatively lower Th/U ratios (1.9 to 7.2; Rao et al., 1972). Sediments with higher Th/U values would have more contribution from uranium-rich mineral deposits in the Mahanadi drainage basin area (2.6 to 11.6; Aswasthanarayana, 1985) and monazites which have very high Th/U ratios (42-52, see Montel et al., 1996). The observed ratios (6.4 to 7.5) in the K-G shelf sediments may also be attributed to the presence of monazite in variable amounts. The presence of monazite-rich beach sands is known from the Waltair, Bimlipatnam, and Narasipatnam regions in the K-G coastal areas (Mohanty et al., 2003). The high Th concentrations in Kaveri shelf sediments may be of local importance due to channels bringing in beach sand to the depositional sites (Mazumdar et al., 2014) and the beach sands of the coastal tracts of Tamil Nadu are known to have monazite (Gujar et al., 1988).

4.4. Rare earth elements as indicators of provenance

Rare-earth elements (REE) are very useful indicators of provenance as it is believed that they are not easily fractionated during the sediment transport and deposition, sedimentary REE patterns may provide an index to average provenance compositions (Taylor and McLennan, 1985). The characteristic REE patterns that describe the fractionation between lighter (LREE) and heavier

REEs (HREE), can be deciphered from shale-normalized ratios (La/Sm, La/Yb) and along with Eu anomaly (Eu/Eu*) have been used as indicators of provenance (McLennan 1989).

The mean total REE concentration (Table 5) in these sediments is higher than the REE content of PAAS (185ppm). Most of the shale-normalized REE sediment patterns observed here are generally flat having a sample/PAAS ratio close to 1 (Fig. 6) and are indicative of a terrigenous source (Nath et al., 1992). The sediments off G-B and Mahanadi shelves show REE patterns enriched in LREE compared to those off K-G and Kaveri shelves. Higher REE content in Mahanadi shelf sediments (up to 907ppm, Table 5) is possibly related to monazite placer deposits which are widespread along the Orissa coast (e.g., Mohanty et al., 2003). Sediments from the Kaveri shelf are dominated by sand fraction (> 90%) which could be the reason for the low total REE content (min. 65 ppm). Low REE content was also reported in Kaveri River sediments (Singh and Rajamani, 2001a). Thus the REE composition has controls of mineralogy and grain size (see Kurian et al., 2013).

The LREE enrichment can reflect source rock signature as well as weathering of source rocks with a resultant increase in the LREEs in the detrital material (Nath et al., 2000). The $(La/Yb)_n$ ratios of the G-B shelf sediments (avg. 1.5) are higher than Mahanadi shelf sediments (avg. 1.36), Kaveri shelf sediments (avg. 1.31) and K-G shelf sediments (avg. 0.82). The variable $(La/Yb)_n$ ratios variation seen on the ECSI sediments for different areas may be due to source rock characteristics sediments. The $(La/Yb)_n$ ratios of the Deccan Basalts range from 0.38 to 0.58 (Melluso et al., 2004), which are markedly different from the $(La/Yb)_n$ ratios of charnockites (avg. 2.05) of low to high-grade metamorphic transition zone from south India (Condie et al., 1982). $(La/Yb)_n$ ratios of ~ 1.07 have also been reported from basic granulites (Rao and Rao, 1988). The Late Archaean granites and tonalities-trondjhemites-granodiorites (TTG) have average $(La/Yb)_n$ ratios of 1.84-2.21 (Condie 1993). Apparently, the Mahanadi and G-B shelf sediments have $(La/Yb)_n$ ratios that reflect a mixture of low to high-grade metamorphic transition zone charnockites and Archaean granites and tonalities-trondjhemites-granodiorites (TTG), whereas comparatively lower $(La/Yb)_n$ ratios in the K-G and Kaveri shelf sediments reflect a significant contribution from the Deccan basalts.

Eu-anomaly, denoted by Eu/Eu* is calculated as Eu-anomaly = PAAS normalized Eu / Mean value of PAAS normalized Sm and Gd. Eu/Eu* in the study area ranges from 0.24 to 1.98 (Fig. 5). The G-B shelf sediments have Eu anomaly between 0.9 and 1.2 which is much higher than the Eu anomaly of 0.2 to 1.1 of Mahanadi shelf sediments. Eu anomaly is generally indicative of sediment source (McLennan et al., 1993) and plagioclase content (Nath et al., 1992) and is less prone to weathering and diagenesis (Taylor and McLennan, 1985). The suspended sediments from the Ganges

and bedload sediments from the Brahmaputra (Ramesh et al., 2000) have an Eu anomaly of 0.8 which is in good agreement with that seen in G-B shelf sediments of the present study. This may be due to the weathering of granites and granitic gneisses in the source region (Burg et al., 1984; Gansser et al., 1983). The Eu/Eu* ratios in the Mahanadi and Kaveri shelf sediments are predominantly >1, except at a few locations, where it was < 1, suggesting the role of feldspar in contributing to the positive Eu anomaly in the sediments. Mahanadi and Kaveri shelf sediments seem to derive their sediments from TTGs, and peninsular granites with a small component derived from the Deccan basalts. The high Eu anomaly in K-G shelf sediments can also be related to the drainage basin lithology. Gneisses and charnockites in south India formed by retrograde metamorphism (Allen et al., 1985) showed similar patterns with positive Eu anomaly (Nath et al., 2000). The K-G shelf sediments consistently show positive Eu anomaly (1.1 to 1.5) indicating a contribution from Deccan traps (Eu/Eu* = 1.42) containing basalts (Eu/Eu* = 1.2 to 1.6) (Melluso et al., 2004; Dessai et al., 2008). The spread in Eu values in the Kaveri shelf sediments suggests a variable source rock composition in the source area.

4.5. Clay minerals as tracers of provenance

The sediments from the ECSI consist of variable concentrations of clay minerals (Fig. 3). Higher concentration of smectite in the southern part (South of 18° N, K-G and Kaveri shelf) of the ECSI than the northern part (North of 18° N, G-B and Mahanadi shelf) is attributed to the derivation of smectite from the Deccan Traps (see Rao, 1964). This is consistent with earlier published clay mineral (Rao, 1991) and the magnetic susceptibility and physical property studies (Sebastian et al., 2019) in the region. South of the G-B and Mahanadi shelf, poorly-drained soils which are conducive to smectite formation are responsible for their occurrence. Smectites are diagnostic of alteration of volcanic or rocks of effusive (basaltic) origins. These findings are comparable with other data sets from the region that similarly show the high smectite content in G-B sediments (Segall and Kuehl, 1992). High smectite abundance has been reported in several other studies in areas dominated by G-B deposition (Sarin et al., 1989; Alam et al., 1993, Segall and Kuehl., 1992; Moslehuddin and Egashira, 1997). The majority of the smectites in the Ganges form from low-temperature alterations of HHSC metasediments during the pedogenic process (France-Lanord et al., 1993). The high smectite content in the K-G shelf sediments with a minor amounts of chlorite and illite (Fig. 3) indicate a variable basaltic source (Das and Krishnaswami, 2007) and support our geochemical data. K-G rivers transport clays very rich in smectite with minor amount of kaolinite and illite. In the K-G drainage basin, the Godavari River drains primarily the upper Deccan basalt province while the Krishna River drains a significant portion of the Archaean-Proterozoic Dharwar granitic complex.

The variable content of smectite and illite in the K-G shelf sediments is possibly due to the relative contribution of the weathering products from Deccan basalt and Archaean rocks (Raman et al., 1995). Mahanadi basin contributes a relatively low amount of smectite with a minor amount of chlorite, kaolinite, and illite. Raman et al. (1995) also reported similar composition with Mahanadi River clays comprising of smectite, kaolinite, and illite.

Illite however shows a reverse trend with the northern portion (north of 18°, G-B and Mahanadi shelf) having higher illite content (Fig. 3). Clay mineral assemblages are strongly influenced by G-B rivers containing abundant illite and chlorite in their suspended load (Rao, 1963). The concentration of illite and chlorite predominates in the soil of northwestern India, which is transported via the G-B rivers to the Bay of Bengal (Rao et al., 1988; Raman et al., 1995). The probable source of this illite must be from the Himalayas. A considerable amount of illite is present with a minor amount of chlorite and kaolinite in the G-B shelf (Fig. 3). Rao (1963) found illite and chlorite with traces of kaolinite while Murthy and Srivastava (1979) reported illite with minor amounts of kaolinite in sediments of Ganges. Illite, kaolinite, and chlorite have been reported in the suspended load, and illite, chlorite in bed loads of the Ganges (Subramanian 1980; Naidu 1985; Datta and Subramanian, 1997). The abundance of illite is related to the dominance of its precursor, the muscovite-type mica in the source rock (Segall and Kuehl, 1992). High contents of illite in the Mahanadi shelf sediments (Table 3; Fig. 3) probably comes from highland rivers draining Precambrian metamorphics, acid intrusives, and Paleozoic-Mesozoic sandstone and shales (Segall and Kuehl, 1992). K-G and Kaveri shelf sediments have intermediate to low amounts of illite indicating a poor contribution.

The kaolinite content also varies in its abundance all along the ECSI (Fig. 3). Kaolinite is primarily a chemical/silicate weathering product, produced by ion-stripping in lower pH environments (Segall and Kuehl, 1992). Relatively high concentrations kaolinite content is seen in Mahanadi and K-G shelf sediments (Fig. 3) compared to the G-B shelf sediments. Rao (1963) found traces of kaolinite in sediments off the Ganges shelf. Kaolinite has been reported in the suspended load of Ganges by Subramanian (1980). Agricultural practices could lead to the formation of high kaolinite concentrations (Segall and Kuehl 1992) and provide an additional supply to the shelf.

The high concentration of chlorite in the G-B shelf sediments (Fig. 3) is likely from upland tributaries during high discharge season (Segall and Kuehl, 1992). The Himalayas are the primary source of chlorite to the study area which is delivered by upland Ganges tributaries and Brahmaputra Rivers during the peak discharge (Segall and Kuehl, 1992). Chlorite is more abundant in the rivers draining the Himalayas than those draining the Indian Peninsula. The occurrence of chlorite is

attributed to the glacial weathering of source rocks in the upper reaches of the G-B rivers (Rao et al., 1988). Mahanadi shelf sediments show very low chlorite content with some locations completely devoid of this mineral. Chlorite derived from Mahanadi is a Fe-rich variety reflecting poor drainage conditions compared to Ganges (Rao et al., 1988). K-G and Kaveri shelf sediments contain a minor amount of chlorite (Fig. 3) but the abundance increases away from the shelf. Raman et al. (1995) reported a virtual absence of chlorite in fluvial suspended and bed loads of the peninsular Indian rivers suggesting that chlorite is not formed under the prevailing climatic regime. The absence of chlorite as well as an abundance of smectite and kaolinite is diagnostic of strong chemical weathering in the peninsular Indian region because of warm and humid climatic conditions. Though the peninsular rivers do not contain chlorite in their bed or suspended sediments, varying amounts of chlorite are found in the adjacent shelf sediments which could either be due to transportation from Ganga's mouth in the north or from the west from chlorite-rich suspensions in the Bay of Bengal (Raman et al., 1995).

4.6. Inferring the weathering intensity in the source regions

A general approach to assess the weathering conditions in the source area is by using the Chemical Index of Alteration (CIA) proposed by Nesbitt and Young (1982) which considers that the major oxides are preferentially lost relative to more refractory alumina during the weathering. CIA is calculated with the formula $[\text{Al}_2\text{O}_3/(\text{Al}_2\text{O}_3 + \text{CaO}^* + \text{Na}_2\text{O}^* + \text{K}_2\text{O})] \times 100$, with each term expressed in molar weight percent, where CaO^* and Na_2O^* represent Ca and Na associated with the silicate fraction only to avoid bias from the calcium from carbonates (Fedo et al., 1995) and the Na from seawater (Nath et al., 2000).

CIA values are reported on a general scale of 40 to 100, with the lowest values found for unweathered felsic rocks (45–55) and fresh feldspars (~50) (Nesbitt and Young, 1982) and highest for residual clays with high content of kaolinite and gibbsite (McLennan, 1993; Nath et al., 2000 and references therein). High CIA values, but lower than kaolinite and gibbsite, are also found in illite, a common clay product of feldspar and mica weathering (75–90, McLennan, 1993). It varies from 70 to 75 in average shales. CIA values for the sediments of the present study area from the ECSI varied between 39 and 81 (Table 4, Fig. 5) with G-B shelf sediments showing similar CIA values (avg. 72) to those of Mahanadi shelf sediments.

High CIA values (~ 72) found in the northern shelf sediments (G-B and Mahanadi) suggest a variable weathering contribution of felsic rocks, which is related to greater illite and kaolinite content (Fig. 3). Residual clays with high amounts of kaolinite exhibit CIA that approach 100, while illite

has CIA values > 70 (Nath et al., 2000). The Mahanadi shelf sediments have an average of 28.5% kaolinite and G-B has average illite content, of 24.5% which is the highest for the ECSI sediments. The Holocene sediments in the Bengal basin also display a similar ratio (50-65, Goodbred et al., 2014). The relatively lower CIA values (avg. 67) in the K-G shelf sediments compared to the Mahanadi shelf (avg. 72) may be due to the variable contribution of Deccan basalt-derived material in the K-G shelf sediments compared to the primarily granitic-derived material in the Mahanadi shelf sediments as the Deccan basalts have low CIA value of ~ 37 (Das and Krishnaswami, 2007). In addition, the southern shelf sediments (K-G and Kaveri) have high smectite content compared to the northern shelf sediments (G-B and Mahanadi) which may be responsible for the low CIA values in the southern shelf sediments. A low degree of chemical weathering is also reported in sediments of the Kaveri River (Singh and Rajamani, 2001a and b). A relative change in provenance is attributed to the observed change in the CIA values (see Kurian et al., 2013 for a similar scenario in the western Indian continental margin). Overall, the CIA values found here for the ECSI are indicative of moderate weathering.

On closer examination of the data shows that the CIA values are higher in the deeper parts of the northern shelf sediments, while the sediments closer to the mouth of the rivers exhibit lower CIA values (Fig. 5). This indicates that CIA values seem to be controlled by the clay content in the sediments. The finer clay particles are transported away from the shelf and tend to get enriched in Al, which explains the high CIA values in offshore sediments. Further, the source sediments for the Kaveri shelf sediments with CIA (39) (present study) plot well below the feldspar join indicating an unweathered nature of the sediments, while the offshore counterpart exhibit deposition of more weathered products (Fig. 8) with loss of Ca and Na and a concomitant gain in Al.

Further evidence of the degree of weathering is seen in the A-CN-K diagram, where there is a progressive increase in silicate weathering from the source sediments to the offshore shelf sediments indicated by relative enrichment of Al_2O_3 and reduction of CaO and Na_2O and K_2O (Fig. 8). Plagioclase is more susceptible to weathering than potassium feldspar, and thus, Ca and Na are leached preferentially over K (Nesbitt and Young, 1982, 1989). Overall, the weathering trend of the studied shelf sediments is parallel to the A-CN line, implying the removal of the Ca and Na-bearing silicate minerals from the parent rocks, with the K-bearing minerals less altered. The shelf sediments of the G-B along with Mahanadi (northern rivers) exhibit relatively higher K_2O and Al_2O_3 compared to the K-G and Kaveri (southern rivers) rivers.

The sediments that represent the source area (collected closest to the coast, in this study) had very high sand content with a maximum going up to 99% (Fig. 2). This either indicates a very high

degree of physical weathering in the terrain or the occurrence of high energy conditions in the depositional site. The clay fraction in the regolith of the Kaveri drainage basin was reported to be uniformly low (Sharma and Rajamani, 2000) with maximum clay content not exceeding 5%. It is rather surprising that although the river catchment area is comparatively small, the CIA values of the shelf sediments range from 39-74. Sediment sorting also could play a role. It is noted that the Kaveri River drains into the Bay of Bengal with a very narrow shelf area which directly transports the coarse-grained sediments to deeper parts of the basin.

4.7. Deciphering dispersal patterns and relative source contributions estimation from modeling studies

While the regional elemental distribution maps and the geochemical discrimination ratios and plots have helped in assessing the provenance and the dispersal patterns from different sources, a quantitative approach was needed to assign the relative contribution of each of these competing sources. For this, a least square minimization technique that uses a mass balance approach is used to iteratively calculate the relative contribution from each of the sources to a site using pre-assigned elemental data for the sources. The model is used to apportion the contributions from five riverine sources viz., G-B, Mahanadi, Godavari, Krishna, and Kaveri (Fig. 9).

The total observed mass of an element (B_i) can be expressed as

$$B_i = \sum_{k=1}^5 A_{ik} \cdot X_k, \quad i = 1, n$$

Where A_{ik} is the concentration of element i (Al, Ti, Fe and Mg) from source k (i.e. end members) and X_k is the relative contribution from each of the individual sources k and n is the number of adopted element. In vector form the above equation becomes $\mathbf{A} \cdot \mathbf{X} = \mathbf{B}$, where \mathbf{A} and \mathbf{B} are obtained from the observations of source and sediments from unknown sources respectively. The relative contribution from each source member given by the components of vector \mathbf{X} is the unknown quantity to be determined here. A model constraint of fractions contributed by each source end member varying between 0 and 1 is used. The bounded-variable least square algorithm (BVLS) by Stark and Parker (1995) is applied to solve this equation. BVLS utilizes “warm-start” strategy similar to non-negative least square algorithm by Lawson and Hanson (1974), but allows the variables to be initialized at their upper and lower bounds. BVLS uses least square approach with QR decomposition to solve the problem.

The shelf sediments closest to the river mouth is used for representing the source of the river to the shelf. Accordingly, 5 samples as shown in Figure 9 were selected. Dispersal patterns are better traced using geochemical data from the clay-sized fraction (Nath et al., 2000). However as we do not have this fraction, we have used geochemical data of sediments with more than 20% clay in the sediments. This helped in removing the effect of high sand content.

Lithogenic elements such as Al, Ti, Fe, and Mg are considered diagnostic of the source because of their varying affinities to felsic and basic rocks (see Kurian et al., 2013). Similar to the western continental margin of India, a provinciality is seen separating Al_2O_3 enriched (mean 16.5%; Fig. 4) and Fe-Ti-Mg-depleted (mean for their oxides being 1.11, 7.5, and 1.88% respectively) sediments in the north of Mahanadi shelf from those depleted in Al_2O_3 (mean 12.32%) and enriched in Fe, Ti and Mg oxides in the south of the Mahanadi shelf (mean 1.2, 8.5 and 2.18%). This distinct provinciality is consistent with the geology of the source terrain (Fig. 1, 4). Therefore we have used these elements as provenance indicators. The priori compositions for the elements of the five sources are shown in Table 6.

The model results on the sediment contributions from source rocks in the drainage basins of G-B, Mahanadi, Godavari, Krishna, and Kaveri rivers to the continental shelf sediments are shown in Fig. 12. Inferring the sediment dispersal pathways in the continental margins of India based on the model results, is to our knowledge the first of its kind. The model distribution map shows a complex sediment dispersal pattern. A clear regional variability in sediment dispersal map is seen with distinct provinciality reflecting the distinct source composition. The dispersal of sediments within the continental shelf is affected primarily by oceanic circulation, local bathymetry, and turbidity currents. The hydrography in the Bay of Bengal is primarily driven by the seasonally changing Indian monsoons. The plot depicting the latitudinal distribution of the model results along with the reversing seasonal currents demarcates the extent of influence of each source area on the ECSI (Fig. 12).

Modeling studies carried out on the sediments indicate that the influence of the G-B River is significantly high at the mouth of the river and progressively decreases southwards to about 50% at 18°N , indicating a reduced influence of the source rocks away from the mouth but not progressing offshore beyond Mahanadi river mouth. While our study shows that the G-B river derived sediments are limited in their spread only until the north of Mahanadi river mouth on the ECSI, the G-B sediments are known to spread to thousands of kilometers towards the south beyond the equator, extending to 8° to 10°S (Nath et al., 1989; 1992) in the Central Indian Basin.

The distribution pattern of the Godavari shelf sediments can be traced on either side of the river mouth which indicates that these sediments are dispersed both towards the northern and southern side. The sediment dispersal patterns seem to be responding to the physical dynamics along the shelf, possibly due to the seasonally reversing East India Coastal Current (EICC). The EICC seems to play an important role, in the sediment transport along the central and south-central parts of the east coast of India (Shankar et al., 2002). The northern limit of the Godavari shelf sediments is seen to extend south of Puri, while the southern limit is seen to extend to Chennai. The provenance of the Krishna shelf sediments is seen along a narrow shelf limited to the south of the river mouth. This marks the end of the influence of the Deccan trap Province on the Eastern continental shelf sediments and the beginning of the peninsular Indian provenance consisting of a mixture of Precambrian granitic gneisses, tonalite-trondjemite gneisses and charnockites of South India. This is consistent with the hydrography of the area. Longshore sediment transport direction, estimated along the Tamil Nadu, Andhra Pradesh and Orissa coast, is highly variable. It is towards the south for four months during November-February, towards the north for six months during April-September and variable during March and October with a net transport towards the north (e.g., Kumar et al., 2006). Annual sediment transport is northerly at Andhra Pradesh and Orissa coasts whereas it is negligible along the Tamil Nadu coast. These results suggest the highly dynamic nature of coastal and longshore currents control the dispersal pattern of fluvial sediments along the ECSI.

5. Conclusions

A first comprehensive geochemical study covering the entire eastern continental shelf of India (ECSI) in the western Bay of Bengal has demonstrated that the sediment chemistry is seen to reflect the lithology of the catchment area of the rivers draining the east coast of India. A clear provinciality is seen in elemental distribution patterns of diagnostic elements viz., the Fe, Al, Ti, and Mg. Major, trace and rare-earth element variations, different geochemical discriminatory plots and diagnostic elemental ratios (including that of Eu/Eu^*) suggest that the sediments from the south (Kaveri shelf) are derived from source rocks containing a mixture of peninsular granitic gneisses, tonalite-trondjemite gneisses and charnockites, while the northern (G-B) shelf sediments are derived from rocks in High Himalaya Crystalline (HCC) sequence and the Tethyan sedimentary series. A higher concentration of the major elements typically separates the K-G shelf from other areas because of their source in the Deccan trap basaltic terrain. Support comes from trace elements and their ratios too. The geochemical data indicate a mixed signature of a mafic contribution probably from the Deccan basalts and felsic contribution of the peninsular granitic and gneissic complex from south India to the Mahanadi and K-G shelf sediments

Weathering indices such as clay mineralogy, CIA and discrimination plots involving oxides of Al, Ca, Na, and K also showed variability in the intensity of weathering but they were also found to be a function of the sediment provenance possibly depending on the different degrees susceptibility of each rock type to weathering, sediment texture and clay mineralogy. In general, the shelf sediments in the south (K-G and Kaveri) show a lower chemical weathering index compared to those from northern shelf sediments (Mahanadi and G-B). A relative change in provenance is attributed to the observed change in the CIA values. CIA values were also found to vary with types of clay minerals present. Northern shelf sediments with greater illite and kaolinite content had higher CIA values compared to lower CIA values in smectite rich southern shelf sediments. Overall, the index values show that these modern/late Holocene sediments from the ECSI have undergone a moderate degree of weathering.

Modeling of the end-member geochemical data revealed a regional variability in sediment dispersal patterns indicating distinctly different source control. Modeling also indicated that the influence of the rivers is significantly high at the mouth and progressively decreases away southwards indicating a reduced influence of the source rocks away from the mouth. Significantly, sediments from mighty G-B are confined to a limited extent on the continental shelf (north of Mahanadi River), unlike their offshore spread to thousands of kilometers beyond the equator. The sediment dispersal patterns seem to be responding to the physical dynamics along the shelf, with hydrography controlling their transport pathways in the ECSI.

Declaration of Competing Interest

The authors declare that they have no known competing financial interests/personal relationships which may be considered to influence the work reported in this paper.

Data availability

All the data used in this paper is presented in Tables.

Acknowledgement

The authors thank Director, CSIR-NIO for providing the ship time and permission to publish. Our sincere thanks are due to Dr. A.V. Mudholkar and Mr. Girish Prabhu for XRD and XRF analyses respectively. All the shipboard scientific staff of *R.V. Sindhu Sankalp* cruises 35 and 50 are sincerely acknowledged for their help during the sediment sample collection. Our sincere thanks to the handling Editor Dr. Adina Paytan and two anonymous reviewers for their thorough and positive reviews. The sediments were collected for the Source to Sink WP of CSIR XII Plan Project GEOSINKS. This is NIO Contribution No.

Author statement

Conceptualization – BNN and MBLMP, Field collection and investigation – MBLMP, BNN, NS, RAR, SA, KA, AMS, PM, PJ, KM, TS, BRR, PG, Data Curation - MBLMP and BNN, Writing - Original Draft - MBLMP, Writing - Review & Editing – BNN and all the authors, Resources and Funding acquisition – BNN

References

- Ahmad, T., Thakur, V. C., Islam, R., Khanna, P. P., & Mukherjee, P. K. (1998). Geochemistry and geodynamic implications of magmatic rocks from the Trans-Himalayan arc. *Geochemical Journal*, 32(6), 383-404.
- Alagarsamy, R., & Zhang, J. (2005). Comparative studies on trace metal geochemistry in Indian and Chinese rivers. *Current Science*, 89.
- Alam, M., Alam, M. M., Curray, J. R., Chowdhury, M. L. R., & Gani, M. R. (2003). An overview of the sedimentary geology of the Bengal Basin in relation to the regional tectonic framework and basin-fill history. *Sedimentary Geology*, 155(3-4), 179-208.
- Aswathanarayana, U. (1985). Principles of Nuclear Geology, Oxodian Press Pvt. Ltd., pp.211-212.
- Ayres, M., & Harris, N. (1997). REE fractionation and Nd-isotope disequilibrium during crustal anatexis: Constraints from Himalayan leucogranites. *Chemical Geology*, 139(1-4), 249-269.
- Bejugam, P., & Nayak, G. N. (2017). Source and depositional processes of the surface sediments and their implications on productivity in recent past off Mahanadi to Pennar River mouths, western Bay of Bengal. *Palaeogeography, Palaeoclimatology, Palaeoecology*, 483, 58-69.
- Biscaye, P. E. (1965). Mineralogy and sedimentation of recent deep-sea clay in the Atlantic Ocean and adjacent seas and ocean. *Geological Society. American Bulletin*, 76, 803–832.
- Bose, M. K. (1972). Deccan basalts. *Lithos*, 5(2), 131-145.
- Brown, R. J., Blake, S., Bondre, N. R., Phadnis, V. M., & Self, S. (2011). A' ā lava flows in the Deccan Volcanic Province, India, and their significance for the nature of continental flood basalt eruptions. *Bulletin of Volcanology*, 73(6), 737-752.
- Burg, J. P., Guiraud, M., Chen, G. M., & Li, G. C. (1984). Himalayan metamorphism and deformations in the North Himalayan Belt (southern Tibet, China). *Earth and Planetary Science Letters*, 69(2), 391-400.
- Chakrapani, G. J. (2005). Factors controlling variations in river sediment loads. *Current Science*, 569-575.
- Chakrapani, G. J., & Subramanian, V. (1990). Preliminary studies on the geochemistry of the Mahanadi river basin, India. *Chemical Geology*, 81(3), 241-253.
- Condie, K. C. (1993). Chemical composition and evolution of the upper continental crust: Contrasting results from surface samples and shales. *Chemical Geology*, 104(1-4), 1-37.

- Condie, K. C., Allen, P., & Narayana, B. L. (1982). Geochemistry of the Archean low-to high-grade transition zone, southern India. *Contributions to Mineralogy and Petrology*, 81(3), 157-167.
- Condie, K. C., & Allen, P. (1984) Origin of Archean chamockites from southern India. In *Archaean Geochemistry* eds. A. Kroner, A. M. Goodwin and G. M. Hanson, Springer-Verl, Berlin.
- Curry, J. R., Emmel, F. J., Moore, D. G., & Raitt, R. W. (1982). Structure, tectonics, and geological history of the northeastern Indian Ocean. In *The ocean basins and margins* (pp. 399-450). Springer, Boston, MA.
- Das, A., & Krishnaswami, S. (2007). Elemental geochemistry of river sediments from the Deccan Traps, India: Implications to sources of elements and their mobility during basalt–water interaction. *Chemical Geology*, 242(1-2), 232-254.
- Das, A., Krishnaswami, S., Sarin, M. M., & Pande, K. (2005). Chemical weathering in the Krishna Basin and Western Ghats of the Deccan Traps, India: Rates of basalt weathering and their controls. *Geochimica et Cosmochimica Acta*, 69(8), 2067-2084.
- Datta, D. K., & Subramanian, V. (1997). Nature of solute loads in the rivers of the Bengal drainage basin, Bangladesh. *Journal of Hydrology*, 198(1-4), 196-208.
- Dessai, A. G., Downes, H., López-Moro, F. J., & López-Plaza, M. (2008). Lower crustal contamination of Deccan Traps magmas: Evidence from tholeiitic dykes and granulite xenoliths from western India. *Mineralogy and Petrology*, 93(3), 243-272.
- Dessert, C., Dupré, B., Gaillardet, J., François, L. M., & Allegre, C. J. (2003). Basalt weathering laws and the impact of basalt weathering on the global carbon cycle. *Chemical Geology*, 202(3-4), 257-273.
- Dube, S. K., Rao, A. D., Sinha, P. C., Murty, T. S., & Bahulayan, N. (1997). Storm surge in the Bay of Bengal and Arabian Sea: The problem and its prediction. *Mausam*, 48(2), pp. 283–304,
- Floyd, P.A., Winchester, J.A., & Park, R.G. (1989). Geochemistry and tectonic setting of Lewisian clastic metasediments from the Early Proterozoic Loch Maree Group of Gairloch, NW Scotland, *Precambrian Research*, 45(1–3), 203-214,
- France-Lanord, C., & Derry, L. A. (1997). Organic carbon burial forcing of the carbon cycle from Himalayan erosion. *Nature*, 390(6655), 65-67.
- Galy, A., & France-Lanord, C. (2001). Higher erosion rates in the Himalaya: Geochemical constraints on riverine fluxes. *Geology*, 29, 23–26, doi: 10.1130/0091-7613(2001)29<0023:HERITH>2.0.CO;2 .
- Galy, V., France-Lanord, C., Beyssac, O., Faure, P., Kudrass, H., & Palhol, F. (2007). Efficient organic carbon burial in the Bengal fan sustained by the Himalayan erosional system. *Nature*, 450(7168), 407-410.
- Gassner, A. (1983). The morphogenic phase of mountain building, in HsüK. J., ed., *Mountain building processes*, London, Academic press, p. 221-228.
- Ghose, N. C. (1976). Composition and origin of Deccan basalts. *Lithos*, 9, 65-73.

- Goodbred Jr, S. L., Paolo, P. M., Ullah, M. S., Pate, R. D., Khan, S. R., Kuehl, S. A., ... & Rahaman, W. (2014). Piecing together the Ganges-Brahmaputra-Meghna River delta: Use of sediment provenance to reconstruct the history and interaction of multiple fluvial systems during Holocene delta evolution. *Bulletin*, 126(11-12), 1495-1510.
- Gujar, A. R., Nath, B. N., & Banerjee, R. (1988). Marine minerals: the Indian perspective. *Mar Mining*.
- Janardhan, A.S., Newton, R.C., & Hansen, E.C. (1983). Transformation of the Peninsular Gneiss to charnockite in southern Karnataka, in Naqvi, S.M., and Rogers, J.J., eds., Precambrian of South India, Proceedings of the Indo-U.S. workshop: Geological Society of India, Memoir 4, p. 417–435.
- Kessarkar, P. M., Rao, V. P., Ahmad, S. M., & Babu, G. A. (2003). Clay minerals and Sr–Nd isotopes of the sediments along the western margin of India and their implication for sediment provenance. *Marine Geology*, 202(1-2), 55-69.
- Kumar, V.S., Pathak, K.C., Pednekar, P., Raju, N.S.N., Gowthaman, R. (2006). Coastal processes along the Indian coastline. *Current Science*, 91, 530–536.
- Kurian, S., Nath, B. N., Kumar, N. C., & Nair, K. K. C. (2013). Geochemical and isotopic signatures of surficial sediments from the western continental shelf of India: Inferring provenance, weathering, and the nature of organic matter. *Journal of Sedimentary Research*, 83(6), 427-442.
- Lawson, C. W. & Hanson, R. J. (1974). Solving Least Squares Problems. John Wiley and Sons, Inc., New York.
- Li, J., Liu, S., Feng, X., Sun, X., & Shi, X. (2017). Major and trace element geochemistry of the mid-Bay of Bengal surface sediments: Implications for provenance. *Acta Oceanologica Sinica*, 36(3), 82-90.
- Lipin, B. R., & McKay, G. A. (Eds.). (2018). *Geochemistry and mineralogy of rare earth elements* (Vol. 21). Walter de Gruyter GmbH & Co KG.
- Liu, J., Zhang, X., Xia, J., Wu, S., She, D., & Zou, L. (2016). Characterizing and explaining spatio-temporal variation of water quality in a highly disturbed river by multi-statistical techniques. *SpringerPlus*, 5, 1-17.
- Loucks, D. (2019). Developed river deltas: Are they sustainable?. *Environmental Research Letters*, 14. 10.1088/1748-9326/ab4165.
- Luo, X., Li, Z., Cai, Y., Yi, C., Zhang, Z., Zhang, Y., & Zhang, Y. (2021). Provenance and Tectonic Setting of Lower Cretaceous Huanhe Formation Sandstones, Northwest Ordos Basin, North-Central China. *Minerals*, 11(12), 1376.
- Mahabaleswar, B., Jayananda, M., Peucat, J. J, Swamy, S. (1995). Archean high-grade complex from Satnur–Halagur–Sivasamudram areas, Karnataka, southern India: Petrogenesis and crustal evolution. *Journal of Geological Society of India*, 45, 33–49.
- Martin H., Moyen, J.-F. (2005). The Archean –Proterozoic transition: Sanukitoid and Closepet type magmatism. *Polskie towarzystwo mineralogiczne – Prace specjalne mineralogical society of Poland – special papers Zeszyt 26*, 26.

- Mazumdar, A., Peketi, A., Joao, H. M., Dewangan, P., & Ramprasad, T. (2014). Pore-water chemistry of sediment cores off Mahanadi Basin, Bay of Bengal: Possible link to deep seated methane hydrate deposit. *Marine and Petroleum Geology*, *49*, 162-175.
- McLennan, S. M. (1989) Rare earth elements in sedimentary rocks: Influence of provenance and sedimentary processes. *Rev. Mineral.* *21*, 116–200.
- McLennan, S. M. (1993). Weathering and global denudation. *The Journal of Geology*, *101*(2), 295-303.
- McLennan, S. M., Taylor, S. R., McCulloch, M. T., & Maynard, J. B. (1990). Geochemical and Nd-Sr isotopic composition of deep-sea turbidites: Crustal evolution and plate tectonic associations. *Geochimica et Cosmochimica Acta*, *54*(7), 2015-2050.
- Melluso, L., Barbieri, M., & Beccaluva, L. (2004). Chemical evolution, petrogenesis, and regional chemical correlations of the flood basalt sequence in the central Deccan Traps, India. *Journal of Earth System Science*, *113*(4), 587-603.
- Milliman, J. D. (2001). Delivery and fate of fluvial water and sediment to the sea: A marine geologist's view of European rivers. *Scientia Marina*, *65*, 121.
- Mir, I. A., Mascarenhas, M. B. L., & Khare, N. (2022). Geochemistry and granulometry as indicators of paleoclimate, weathering, and provenance of sediments for the past 1, 00,000 years in the eastern Arabian Sea. *Journal of Asian Earth Sciences*, *227*, 105102.
- Mohanty, A. K., Vijayan, V., Sengupta, D., Das, S. K., & Saha, S. K. (2003). Geochemical characteristics of Ilmenite sands of Chhatrapur beach placer deposit of Orissa, India: A PIXE study. *Internat. Jour. PIXE*, *13*, 121-131.
- Mohanty, P. K., Pradhan, Y., Nayak, S. R., Panda, U. S., & Mohapatra, G. N. (2008). Sediment dispersion in the Bay of Bengal. In *Monitoring and modeling lakes and coastal environments* (pp. 50-78). Springer, Dordrecht.
- Montel, J. M., Foret, S., Veschambre, M., Nicollet, C., & Provost, A. (1996). Electron microprobe dating of monazite. *Chemical Geology*, *131*(1-4), 37-53.
- Morey, G. B., & Setterholm, D. R. (1997). Rare earth elements in weathering profiles and sediments of Minnesota; implications for provenance studies. *Journal of Sedimentary Research*, *67*(1), 105-115.
- Moslehuddin, A. Z. M., Salma, L., & Egashira, K. (1997). Fertility status of Bangladesh soils-A review. *J. Fat. Agr., Kyushu Univ.*, *41*(3.4), 257-267
- Murthy, M. R., & Srivastava, P. C. (1979). Clay mineralogy of shelf sediments of north-west Bay of Bengal. *Marine Geology*, *31*, M21-M32.
- Naidu A. S., Mowatt, T. C., Somayajulu, B. L. K., & Rao, K. S. (1985) Characteristics of clay minerals in the bed loads of major rivers of India. In *Proc. 3rd Intl. Workshop on Transport of Carbon and Minerals in Major Rivers*. pp. 559-568. SCOPE/ UNEP, Hamburg.
- Nath, B. N., Balaram, V., Sudhakar, M., & Plüger, W. L. (1992). Rare earth element geochemistry of ferromanganese deposits from the Indian Ocean. *Marine Chemistry*, *38*(3-4), 185-208.

- Nath, B. N., Bau, M., Rao, B. R., Rao, & Ch. M. (1997). Trace and rare earth elemental variation in Arabian Sea sediments through a transect across the oxygen minimum zone. *Geochimica et Cosmochimica Acta*, 61, 2375–2388.
- Nath, B. N., Gupta, S. M., Mislankar, P. G., Rao, B. R., Parthiban, G., Roelandts, I., & Patil, S. K. (2005). Evidence of Himalayan erosional event at approx. 0.5 Ma from a sediment core from the equatorial Indian Ocean in the vicinity of ODP Leg 116 sites. *Deep–Sea Res. II.*, 52, 2061–2077.
- Nath, B. N., & Iyer, S. D. (1989). Basalt microlapilli in deep sea sediments of Indian Ocean in the vicinity of Vityaz fracture zone. *J. Geol. Soc. India.*, 34, 303-309.
- Nath, B. N., Kunzendorf, H., & Pluger, W. L. (2000). Influence of provenance, weathering, and sedimentary processes on the elemental ratios of the fine-grained fraction of the bedload sediments from the Vembanad Lake and the adjoining continental shelf, southwest coast of India. *Journal of Sedimentary Research*, 70(5), 1081-1094.
- Nesbitt, H. W., & Young, G. M. (1989). Formation and diagenesis of weathering profiles. *The Journal of Geology*, 97(2), 129-147.
- Nesbitt, H., & Young, G. M. (1982). Early Proterozoic climates and plate motions inferred from major element chemistry of lutites. *Nature*, 299(5885), 715-717.
- Paropkari, A. L. (1990). Geochemistry of sediments from the Mangalore-Cochin shelf and upper slope off southwest India: Geological and environmental factors controlling dispersal of elements. *Chemical Geology*, 81(1-2), 99-119.
- Pattan, J. N., Parthiban, G., PrakashBabu, C., Khadge, N. H., Paropkari, A. L., & Kodagali, V. N. (2008). A note on geochemistry of surface sediments from Krishna-Godavari basin, East Coast of India. *J. Geol. Soc. India*, 71(1), 107–114.
- Peng, Z. X., Mahoney, J. J., Hooper, P. R., Macdougall, J. D., & Krishnamurthy, P. (1998). Basalts of the northeastern Deccan Traps, India: Isotopic and elemental geochemistry and relation to southwestern Deccan stratigraphy. *Journal of Geophysical Research: Solid Earth*, 103(B12), 29843-29865.
- Poulton, S. W., & Raiswell, R. (2002). The low-temperature geochemical cycle of iron: From continental fluxes to marine sediment deposition. *American Journal of Science*, 302(9), 774-805.
- Rajamani, V., Tripathi, J. K., & Malviya, V. P. (2009). Weathering of lower crustal rocks in the Kaveri river catchment, southern India: Implications to sediment geochemistry. *Chemical Geology*, 265(3-4), 410-419.
- Raman, C. V., Krishna Rao, G., Reddy, K. S. N., & Ramesh, M. V. (1995). Clay mineral distributions in the continental shelf sediments between the Ganges mouths and Madras, east coast of India. *Continental Shelf Research*, 15, 1773–1793
- Ramesh, R., Ramanathan, A. L., Ramesh, S., Purvaja, R., & Subramanian, V. (2000). Distribution of rare earth elements and heavy metals in the surficial sediments of the Himalayan river system. *Geochemical Journal*, 34(4), 295-319.
- Ramesh, R., Subramanian, V., Grieken, R.V., & Dack, L.V. (1989). The elemental chemistry of sediments in the Krishna River basin, India. *Chemical Geology*, 74, 331-341.

- Rao, V. P. (1991). Clay mineral distribution in the continental shelf sediments from Krishna to Godavari river mouth, east coast of India. *Indian Journal Marine Science*, 20, 7-12.
- Rao, V. P., Reddy, N. P., & Rao, Ch. M. (1988). Clay mineral distribution in the shelf sediments off the northern part of the east coast of India. *Continental Shelf Research*, 8(2), 145–151.
- Rao, M. S. (1963). Clay mineral composition of shelf sediments off the east coast of India. In *Proceedings of the Indian Academy of Sciences-Section A*, Springer India, 58, 1, 6-15.
- Rao, M. S. (1964). Some aspects of continental shelf sediments off the east coast of India. *Marine Geology*, 1(1), 59-87.
- Rao, V. D., Aswathanarayana, U., & Qureshy, M. N. (1972). Trace element geochemistry of parts of the Closepet granite, Mysore State, India. *Mineralogical magazine*, 38, 678-86.
- Roonwal, G. S., Glasby, G. P., & Chugh, R. (1997). Mineralogy and geochemistry of surface sediments from the Bengal Fan, Indian Ocean. *Journal of Asian Earth Sciences*, 15(1), 33-41.
- Sarin, M. M., Krishnaswami, S., Dilli, K., Somayajulu, B. L. K., & Moore, W. S. (1989). Major ion chemistry of the Ganga-Brahmaputra river system: Weathering processes and fluxes to the Bay of Bengal. *Geochimica et Cosmochimica Acta*, 53(5), 997-1009.
- Sastri, V. V., Venkatachala, B. S., & Narayanan, V. (1981). The evolution of the east coast of India. *Palaeogeography, Palaeoclimatology, Palaeoecology*, 36(1-2), 23-54.
- Sebastian, T., Nath, B. N., Venkateshwarlu, M., Miriyala, P., Prakash, A., Linsy, P., Kocherla, M., Kazip, A., & Sijinkumar, A. V. (2019). Impact of the Indian Summer Monsoon variability on the source area weathering in the Indo-Burman ranges during the last 21 kyr—A sediment record from the Andaman Sea. *Palaeogeography, Palaeoclimatology, Palaeoecology*, 516, 22-34.
- Segall, M. P., & Kuehl, S. A. (1992). Sedimentary processes on the Bengal continental shelf as revealed by clay-size mineralogy. *Continental Shelf Research*, 12(4), 517-541.
- Seralathan, P., & Seetharamaswamy, A. (1987). Geochemistry of the modern deltaic sediments of the Cauvery River, east coast of India. *Indian Journal Marine Science*, 16, 31–38
- Shankar, D., Vinayachandran, P.N., Unnikrishnan, A. S., & Shetye, S.R. (2002). The monsoon current in the north Indian Ocean. *Progr. Oceanogr*, 52(1), 63-119.
- Sharma, A., & Rajamani, V. (2000). Weathering of gneissic rocks in the upper reaches of Cauvery river, south India: Implications to neotectonics of the region. *Chemical Geology*, 166(3-4), 203-223.
- Siddique, H. N. (1967). Recent sediments of Bay of Bengal. *Marine Geology*, 5, 249-291.
- Singh, P. (2009). Major, trace and REE geochemistry of the Ganga River sediments: Influence of provenance and sedimentary processes. *Chemical Geology*, 266(3-4), 242-255.
- Singh, P. (2010). Geochemistry and provenance of stream sediments of the Ganga River and its major tributaries in the Himalayan region, India. *Chemical Geology*, 269(3-4), 220-236.

- Singh, P., & Rajamani, V. (2001). REE geochemistry of recent clastic sediments from the Kaveri floodplains, southern India: Implication to source area weathering and sedimentary processes. *Geochimica et Cosmochimica Acta*, 65(18), 3093-3108.
- Singh, S. K., Rai, S. K., & Krishnaswami, S. (2008). Sr and Nd isotopes in river sediments from the Ganga Basin: Sediment provenance and spatial variability in physical erosion. *Journal of Geophysical Research: Earth Surface*, 113(F3).
- Stähle, H.J., Raith, M., Hoernes, S., & Delfs, A., (1987). Element mobility during incipient granulite formation at Kabbaldurga, southern India. *Journal of Petrology*, 28, 803-834.
- Stark, P. B., & Parker, R. L. (1995). Bounded-variable least-squares: an algorithm and applications, *Computational Statistics*, 10, 129-141.
- Subba Rao, M. (1964). Some aspects of continental shelf sediments of the east coast of India. *Marine Geology*, 1, 59-87.
- Subramanian, V. (1980). Mineralogical input of suspended matter by Indian rivers into the adjacent areas of the Indian Ocean. *Marine Geology*, 36(3-4), M29-M34.
- Subramanian, V., & Mohanachandran, G. (1990). Heavy metals distribution and enrichment in the sediments of southern east coast of India. *Marine Pollution Bulletin*, 21(7), 324-330.
- Subramanian, V., Van'tDack, L., & Van Grieken, R. (1985). Chemical composition of river sediments from the Indian sub-continent. *Chemical Geology*, 48(1-4), 271-279.
- Symphonia, K. T., & Nathan, D. S. (2018). Geochemistry and distribution of sediments in the East Indian shelf, SW Bay of Bengal: Implications on weathering, transport and depositional environment. *Journal of Earth System Science*, 127(7), 1-18.
- Syvitski, J.P.M., Kettner, A.J., Overeem, I., Hutton, E.W.H., Hannon, M.T., Brakenridge, G.R., Day, J., Vörösmarty, C., Saito, Y., Giosan, L., Nicholls, R.J. (2009). Sinking deltas due to human activities. *Nat. Geosci.*, 2(10), 681–689. doi:<http://dx.doi.org/10.1038/ngeo629>.
- Taylor, S. R. & McLennan, S. M. (1985). *The Continental Crust: Its Composition and Evolution*. Blackwell Publ., Oxford, 312 pp.
- Taylor, S. R., McLennan, S. M., & McCulloch, M. T. (1983) Geochemistry of Loess, continental crustal composition and crustal model ages. *Geochimica et Cosmochimica Acta*, 47, 1897–1905.
- Tripathy, G. R., Singh, S. K., & Ramaswamy, V. (2014). Major and trace element geochemistry of Bay of Bengal sediments: Implications to provenances and their controlling factors. *Palaeogeography, Palaeoclimatology, Palaeoecology*, 397, 20-30.
- Vaithiyanathan, P., Ramanathan, A. L., & Subramanian, V. (1992). Sediment transport in the Cauvery River basin: Sediment characteristics and controlling factors. *Journal of Hydrology*, 139(1-4), 197-210.
- Veerasingham, S., Venkatachalapathy, R., & Ramkumar, T. (2014). Historical environmental pollution trend and ecological risk assessment of trace metals in marine sediments off Adyar estuary, Bay of Bengal, India. *Environmental Earth Sciences*, 71(9), 3963-3975.

Vital, H., & Stattegger, K. (2000). Major and trace elements of stream sediments from the lowermost Amazon River. *Chemical Geology*, *168*(1-2), 151-168.

Wijayananda, N. P., & Cronan, D. S. (1994). The geochemistry and mineralogy of marine sediments from the eastern Indian Ocean. *Marine Geology*, *117*(1-4), 275-285.

Zhang, M., Yu, Y., Choi, J., Cai, K., & Shi, M. (2020). Petrography and geochemistry of clastic sedimentary rocks as evidence for the provenance of the Jurassic stratum in the Daqingshan area. *Open Geosciences*, *12*(1), 1350-1368.

Table 1: Details of the catchment area and source rock for the eastern continental shelf sediments.

River	Area drained	Source rocks
Ganges-Brahmaputra	Ganges flow through China, Nepal, Bhutan and 11 northern states of India including the Alluvial plains of these states and Bangladesh, while Brahmaputra flows through Tibet (China), Northeastern India, and Bangladesh.	Higher Himalayan crystalline series (HHCS), Lesser Himalayas (LH), Trans-Himalayan batholiths (THB), Tethyan Sedimentary series (TSS), and Alluvial soils
Mahanadi	Chhattisgarh, Odisha and small part of Jharkhand, Maharashtra, and Madhya Pradesh.	Late Archaean and early Proterozoic granite batholiths, tonalite-trondjemite gneisses (TTGs), and charnockites and khondalites. Sedimentary rocks such as the limestone, shale and sandstone and recent alluvium/littoral deposits.
Krishna	Maharashtra, Karnataka, Andhra Pradesh, and Telangana.	Archaean and Younger crystalline rocks (78%), with considerable contribution from the Tertiary Deccan Traps (20%), and recent alluvial (2%) cover
Godavari	Maharashtra, Telangana, Andhra Pradesh, Chhattisgarh and Odisha in addition to smaller parts in Madhya Pradesh, Karnataka, and Union territory of Puducherry.	Deccan trap basalts, late Archaean/early Proterozoic granites, Precambrian and Gondwana sedimentary rocks and recent alluvial cover
Kaveri	Southeastern part of Peninsular India covering states of Karnataka, and Tamil Nadu.	metamorphic (Peninsular granite gneiss, charnockite etc.) and igneous (Closepet granite) terrains belonging to the Precambrian formations of South India

Table 2: Details of sample locations and water depths.

Cruise no	Station name	Latitude (°N)	Longitude (°E)	Depth (m)	No of samples
Ganges Brahmaputra Shelf					
SSK 35	SPC-1	21°06.819	89°01.118	31	14
	SPC-2	21°03.671	89°01.112	49	
	SPC-3A	20°56.475	89°01.400	104.5	
	SPC-4	20°59.939	88°41.803	29	
	SPC-5	20°56.491	88°41.608	44	
	SPC-6	20°55.528	88°30.068	35.5	
	SPC-7	20°40.683	88°30.108	120	
	SPC-8	20°50.904	88°42.233	94	
	SPC-9	20°50.550	88°30.209	78.5	
	SPC-10	20°57.375	88°00.047	31	
	SPC-11	20°51.084	88°00.234	59.5	
	SPC-12	20°42.699	88°00.263	83	
	SPC-13	20°41.219	87°38.599	54	
	SPC-14	20°56.647	87°40.005	42	
Mahanadi Shelf					
SSK 35	SPC-15	20°52.059	87°24.759	36	21
	SPC-16	20°38.959	87°16.189	28	
	SPC-17	20°11.754	86°52.348	34	
	SPC-18	20°05.786	86°56.847	54	
	SPC-19	20°02.768	86°59.248	96	
	SPC-20	19°48.684	86°33.248	107	
	SPC-21	19°52.040	86°30.399	47	
	SPC-22	19°54.837	86°27.870	36	
	SPC-23	19°19.419	85°05.673	33.5	
	SPC-24	19°17.213	85°07.575	55	
	SPC-25	19°09.844	85°14.853	106	
	SPC-26	18°51.282	85°00.675	122	
	SPC-27	19°00.550	84°49.774	55	
	SPC-28	18°09.402	84°22.090	99.5	
	SPC-29	18°15.117	84°14.939	54	
	SPC-30	18°18.082	84°11.849	36	
	SPC-31	18°07.52085	83°59.25484	33.3	
	SPC-32	18°03.161	84°02.137	55	
	SPC-33	17°35.378	83°43.671	114	
	SPC-34	17°45.166	83°34.045	54	
	SPC-35	17°50.422	83°31.000	31	
Godavari Shelf					
	SPC-36	16°28.542	82°20.604	145	3

	SPC-37	16°15.398	81°59.446	44	
	SPC-38	16°09.980	81°43.981	52	
	Krishna Shelf				
	SPC-39	15°49.731	81°15.405	62	3
	SPC-40	15°42.460	81°04.930	53	
	SPC-41	15°35.268	80°51.609	69	
	Kaveri Shelf				
	SPC-42	12°21.230	80°18.838	56	24
	SPC-43	12°30.937	80°22.620	52	
	SPC-44	12°30.9518	80°14.490	33	
	SPC-45	12°41.049	80°34.469	107	
	SPC-46	12°43.485	80°40.471	190	
SSK 50	SPC-6	12° 55.10	80° 40.14	238	
	SPC-7	12° 59.52	80° 37.57	202	
	SPC-8	13° 4.90	80° 36.04	199	
	SPC-9	12° 40.61	80° 37.79	148	
	SPC-10	12° 41.71	80° 27.60	77.8	
	SPC-11	11° 49.40	79° 53.07	25.7	
	SPC-12	11° 49.27	79° 56.48	56.6	
	SPC-13	11° 23.27	79° 56.48	56.6	
	SPC-14	11° 23.31	79° 57.53	81.9	
	SPC-15	11° 23.49	79° 52.56	35	
	SPC-16	10° 49.65	80° 4.68	51.5	
	SPC-17	10° 49.63	80° 1.09	31.6	
	SPC-20	10° 40.97	80° 14.05	182	
	SPC-21	10° 50.14	80° 14.09	197	
SPC-22	10° 50.74	80° 18.34	345		
SPC-23	10° 50.83	80° 21.81	522		
SPC-24	13° 30.06	80° 26.46	51.6		
SPC-25	13° 29.97	80° 29.21	76.6		
SPC-26	14° 0.45	80° 22.56	61		

Table 3: Textural parameters and clay mineral content of surface sediments from the eastern continental shelf of India. (All values in %).

Cruise	SPC	Sand	Silt	Clay	Smectite	Illite	Kaolinite	Chlorite	
Ganges Brahmaputra Shelf									
SSK 35	1	6.9	53.1	40.0	42.1	33.3	12.1	12.5	
	2	10.1	59.9	30.0	36.9	35.2	13.2	14.7	
	3A	0.3	59.3	40.4	59.6	21.2	7.6	11.6	
	4	11.0	54.3	34.8	58.5	21.6	13.3	6.6	
	5	8.4	55.4	36.2	61.5	19.5	9.6	9.4	
	6	10.6	59.3	30.1	91.4	2.9	4.0	1.7	
	7	0.6	47.3	52.2	53.6	25.4	10.1	10.8	
	8	0.9	61.3	37.8	55.2	24.6	10.1	10.2	
	9	4.1	56.9	39.0	46.0	28.8	14.6	10.6	
	10	30.1	45.4	24.5	57.5	20.0	11.3	11.1	
	11	74.8	13.1	12.2	66.9	16.5	8.9	7.7	
	12	0.2	54.3	45.5	43.7	30.5	12.7	13.2	
	13	47.8	24.5	27.8	47.2	30.5	12.2	10.1	
	14	79.9	10.3	9.8	45.6	33.2	9.8	11.5	
	Avg.	20.4	46.7	32.9	54.7	24.5	10.7	10.1	
	Min	0.2	10.3	9.8	36.9	2.9	4.0	1.7	
	Max	79.9	61.3	52.2	91.4	35.2	14.6	14.7	
	Mahanadi Shelf								
	15	95.0	2.4	2.5	36.6	40.7	9.2	13.4	
	16	4.2	41.2	54.7	50.1	16.3	33.6	0.0	
	17	38.6	31.1	30.3	56.3	16.0	27.8	0.0	
	18	6.5	55.0	38.5	39.7	19.4	40.9	0.0	
	19	0.9	54.8	44.3	67.0	13.0	20.0	0.0	
	20	1.0	48.7	50.3	53.2	16.7	17.1	13.0	
	21	5.5	48.3	46.3	38.8	17.4	43.9	0.0	
	22	49.7	24.2	26.2	43.7	23.2	33.1	0.0	
	23	80.4	7.3	12.3	49.9	13.1	37.0	0.0	
	24	4.2	43.9	51.9	50.6	20.9	28.5	0.0	
	25	5.8	33.2	61.1	54.0	14.9	23.6	7.5	
	26	72.9	13.8	13.4	65.8	14.6	19.6	0.0	
27	90.9	4.1	5.0	60.6	13.9	25.5	0.0		
28	79.1	8.2	12.8	69.3	14.1	12.9	3.7		
29	51.9	25.4	22.8	54.2	15.9	29.9	0.0		
30	29.8	44.3	25.9	52.4	9.1	38.5	0.0		
31	23.1	47.5	29.4	45.4	17.6	37.1	0.0		
32	13.9	45.2	40.9	52.9	15.3	31.7	0.0		
33	84.8	9.0	6.2	55.1	21.0	19.8	4.1		
34	4.7	46.6	48.7	49.4	14.7	35.9	0.0		
35	96.5	1.8	1.8	49.2	16.9	33.9	0.0		
Avg.	40.0	30.3	29.8	52.1	17.4	28.5	2.0		
Min	0.9	1.8	1.8	36.6	9.1	9.2	0.0		
Max	96.5	55.0	61.1	69.3	40.7	43.9	13.4		

		Godavari Shelf							
SSK-50	36	0.8	47.7	51.6	73.7	5.9	20.4	0.0	
	37	3.1	45.8	51.0	81.9	4.5	13.6	0.0	
	38	1.9	42.7	55.4	62.4	8.1	29.5	0.0	
	Avg.	2.0	45.4	52.7	72.7	6.2	21.1	0.0	
	Min	0.8	42.7	51.0	62.4	4.5	13.6	0.0	
	Max	3.1	47.7	55.4	81.9	8.1	29.5	0.0	
			Krishna Shelf						
	39	7.9	50.7	41.4	54.8	24.3	9.7	11.2	
	40	2.4	51.3	46.4	89.1	5.6	4.8	0.5	
	41	0.4	23.6	76.0	96.9	0.0	1.9	1.2	
	Avg.	3.6	41.9	54.6	80.2	10.0	5.5	4.3	
	Min	0.4	23.6	41.4	54.8	0.0	1.9	0.5	
	Max	7.9	51.3	76.0	96.9	24.3	9.7	11.2	
			Kaveri Shelf						
	42	92.2	4.3	3.5	46.5	20.9	24.4	8.1	
	43	95.5	1.8	2.8	65.7	21.9	7.8	4.6	
	44	68.9	20.2	11.0	81.6	3.9	14.5	0.0	
	45	95.3	2.3	2.5	78.1	10.4	9.9	1.6	
	46	69.4	12.5	18.1	71.3	13.6	10.5	4.6	
	6	19.1	39.8	41.1	99.8	0.1	0.1	0.0	
	7	50.4	16.1	33.5	86.1	6.6	5.8	1.6	
8	46.3	21.1	32.6	84.2	6.9	4.8	4.2		
9	75.9	9.1	15.0	85.4	4.8	8.3	1.6		
10	80.4	7.3	12.4	84.0	3.2	12.8	0.0		
11	97.6	1.6	0.9	NA	NA	NA	NA		
12	57.0	35.0	7.9	69.2	8.2	22.6	0.0		
13	57.6	25.6	16.7	80.9	0.0	19.1	0.0		
14	91.0	6.8	2.3	76.7	5.4	17.9	0.0		
15	6.0	48.8	45.2	77.5	2.1	20.4	0.0		
16	90.0	3.7	6.3	41.9	14.4	43.7	0.0		
17	98.8	0.6	0.7	55.2	5.8	39.0	0.0		
20	85.0	4.8	10.2	48.0	12.2	39.8	0.0		
21	74.4	6.9	18.7	74.0	4.4	21.6	0.0		
22	4.2	57.1	38.7	NA	NA	NA	NA		
23	17.0	44.3	38.8	72.9	7.1	20.0	0.0		
24	69.6	16.7	13.8	70.2	10.0	19.9	0.0		
25	62.5	23.1	14.5	NA	NA	NA	NA		
26	7.0	48.4	44.3	85.1	5.0	9.9	0.0		
Avg.	62.9	19.1	18.0	73.1	8.0	17.7	1.2		
Min	4.2	0.6	0.7	41.9	0.0	0.1	0.0		
Max	98.8	57.1	45.2	99.8	21.9	43.7	8.1		

- **BD** Below detection
- **NA** Not analyzed

Table 4: Major (%), trace elemental (ppm) concentrations and chemical index of alteration (CIA) of surface sediments from the eastern continental shelf of India.

Cruise	SPC	SiO ₂	Al ₂ O ₃	TiO ₂	Fe ₂ O ₃	MnO	MgO	CaO	Na ₂ O	K ₂ O	P ₂ O ₅	CIA	Sc	Cr	Co	Ni	Th	U	
SSK 35	Ganges Brahmaputra Shelf																		
	1	58.93	19.51	0.91	7.57	0.05	2.55	0.77	0.83	3.47	0.14	74.99	16.28	108	20.91	56.80	20.70	2.57	
	2	59.23	19.59	0.89	7.55	0.05	2.63	0.77	0.87	3.56	0.15	74.58	17.18	95.51	18.75	61.02	19.55	2.45	
	3A	60.56	19.04	0.89	6.90	0.05	2.62	0.78	1.04	3.69	0.14	72.79	17.18	98.17	17.39	63.23	20.92	2.60	
	4	66.30	16.60	0.84	5.97	0.05	2.20	0.96	1.14	3.28	0.14	69.83	13.42	68.29	13.34	33.96	20.64	2.27	
	5	62.94	17.97	0.85	6.66	0.05	2.41	0.85	0.98	3.44	0.14	72.34	15.34	92.66	15.81	49.62	19.56	2.21	
	6	64.83	17.27	0.86	6.42	0.04	2.26	0.79	1.02	3.34	0.14	71.99	11.33	97.77	13.53	49.92	18.81	2.23	
	7	48.99	22.39	0.87	9.82	0.05	2.83	1.36	0.44	3.27	0.20	76.87	14.89	124	18.00	77.58	18.27	3.32	
	8	61.24	18.72	0.88	7.02	0.05	2.49	0.79	0.95	3.55	0.14	73.24	13.27	104	17.36	67.09	17.05	2.26	
	9	61.35	18.80	0.87	7.04	0.05	2.54	0.82	0.97	3.50	0.14	73.21	14.69	93.81	16.54	57.16	19.52	2.39	
	10	72.70	13.80	0.77	5.03	0.04	1.63	1.01	1.24	2.69	0.15	67.04	13.08	54.70	12.65	28.13	27.84	2.98	
	11	63.02	17.91	0.88	6.71	0.05	2.27	0.81	0.97	3.31	0.14	72.93	12.54	102	16.11	53.53	19.70	2.69	
	12	58.05	19.83	0.92	7.72	0.05	2.61	0.81	0.77	3.62	0.14	74.89	16.61	90.55	18.49	59.46	19.76	3.33	
	13	71.45	13.38	0.73	5.79	0.04	1.77	1.12	0.96	2.94	0.15	66.27	13.81	78.72	17.21	41.03	18.59	2.15	
	14	81.31	8.04	0.61	3.74	0.04	1.02	0.84	0.59	2.04	0.07	63.14	10.68	51.55	12.44	35.13	11.81	1.47	
	Avg.	63.64	17.35	0.84	6.71	0.05	2.27	0.89	0.91	3.26	0.14	71.72	14.31	90.03	16.32	52.40	19.48	2.5	
	Min	48.99	8.04	0.61	3.74	0.04	1.02	0.77	0.44	2.04	0.07	63.14	10.68	51.55	12.44	28.13	11.81	1.5	
	Max	81.31	22.39	0.92	9.82	0.05	2.83	1.36	1.24	3.69	0.20	76.87	17.18	124	20.91	77.58	27.84	3.3	
	Mahanadi Shelf																		
	15	86.59	5.98	1.03	4.37	0.05	0.99	0.80	0.58	1.86	0.07	57.58	6.28	37.75	12.74	17.62	13.32	0.96	
	16	58.63	19.59	1.00	8.58	0.05	1.81	0.72	0.53	2.76	0.14	79.15	17.27	111	18.50	71.30	20.71	2.55	
	17	72.79	13.61	0.85	5.22	0.04	1.49	0.94	1.02	2.95	0.12	67.40	11.86	62.81	12.87	29.82	23.64	2.50	
	18	63.47	17.44	0.93	7.06	0.04	1.98	0.78	0.83	3.04	0.14	74.18	18.26	102	17.53	60.27	22.41	2.87	
	19	60.57	18.66	0.90	7.44	0.05	2.25	0.79	0.81	3.20	0.15	74.98	14.80	97.60	16.82	60.45	19.28	2.72	
20	56.35	20.15	0.96	8.67	0.05	2.13	0.61	0.52	2.97	0.15	79.55	24.52	136	22.26	85.67	21.08	3.24		
21	59.35	19.03	1.03	8.40	0.04	1.78	0.60	0.60	2.85	0.14	78.67	12.45	119	19.80	60.14	20.21	3.13		
22	56.66	19.93	1.05	9.25	0.06	1.49	0.51	0.45	2.71	0.15	81.23	22.95	141	24.24	84.35	25.42	2.92		
23	71.63	10.44	4.16	9.47	0.13	1.22	0.83	0.42	1.89	0.14	71.14	23.64	84	16.56	17.43	133	4.62		
24	59.80	18.80	1.03	8.18	0.04	1.64	0.69	0.52	3.05	0.15	77.68	15.99	113	18.56	62.54	23.31	3.20		

	25	53.48	21.18	0.98	9.41	0.04	2.03	1.07	0.34	2.81	0.17	79.27	22.36	116	21.01	75.46	22.31	4.75	
	26	51.71	19.13	0.91	9.92	0.04	2.54	1.98	0.43	2.81	0.35	72.25	7.35	53.88	25.34	28.05	7.82	2.70	
	27	68.06	14.62	1.10	6.85	0.04	1.35	0.97	0.57	2.95	0.14	71.28	17.93	102	18.57	54.61	60.39	3.20	
	28	53.88	16.20	1.38	12.45	0.07	2.77	1.80	0.35	2.30	0.34	71.87	16.43	92.34	27.05	48.85	18.62	2.78	
	29	74.37	11.74	1.51	6.47	0.06	1.18	0.93	0.52	2.63	0.12	68.51	16.32	85.77	18.12	41.12	44.47	2.50	
	30	68.15	14.89	1.27	7.35	0.05	1.04	0.65	0.44	2.90	0.13	74.70	16.97	86.81	17.98	44.50	32.60	2.35	
	31	68.14	16.33	1.12	5.88	0.04	0.76	0.66	0.64	4.05	0.14	71.12	13.50	76.55	17.27	35.85	29.33	2.22	
	32	62.26	17.31	1.08	7.89	0.04	1.36	0.84	0.51	3.16	0.17	74.91	19.97	109	21.86	63.99	21.04	2.50	
	33	44.42	14.11	0.77	11.90	0.03	2.14	6.39	0.35	2.07	0.60	49.42	9.26	57.46	31.65	34.71	9.69	4.32	
	34	58.03	18.88	1.03	8.72	0.04	1.44	0.75	0.43	3.04	0.17	77.91	16.90	107	21.61	62.48	16.80	2.82	
	35	82.38	6.85	3.09	6.40	0.10	0.82	0.85	0.58	1.72	0.10	61.15	12.59	41.78	11.16	11.35	47.05	1.42	
	Avg.	63.37	15.95	1.29	8.09	0.05	1.63	1.15	0.54	2.75	0.18	72.09	16.08	91.97	19.60	50.03	30.10	2.87	
	Min	44.42	5.98	0.77	4.37	0.03	0.76	0.51	0.34	1.72	0.07	49.42	6.28	37.75	11.16	11.35	7.82	0.96	
	Max	86.59	21.18	4.16	12.45	0.13	2.77	6.39	1.02	4.05	0.60	81.23	24.52	141	31.65	85.67	133	4.75	
	Krishna-Godavari Shelf																		
	36	52.69	18.22	1.50	11.44	0.11	2.35	1.31	0.41	1.78	0.18	78.49	23.69	123	27.37	81.22	14.16	1.89	
	37	56.32	16.00	2.01	10.88	0.08	2.40	2.31	0.84	1.65	0.17	68.49	22.62	106	33.40	62.50	14.63	2.13	
	38	56.96	16.04	2.14	10.84	0.07	2.35	2.08	0.88	1.56	0.16	69.86	25.50	114	29.94	73.84	13.58	2.01	
	39	57.17	14.01	3.11	11.41	0.10	2.74	3.64	1.33	1.23	0.15	58.01	22.88	114	37.74	66.01	9.92	1.54	
	40	56.25	14.58	2.67	11.25	0.10	2.81	3.48	1.20	1.21	0.16	60.25	25.82	123	37.45	75.87	10.18	1.56	
	41	55.32	14.93	2.41	11.17	0.10	2.87	2.99	0.92	1.24	0.16	64.35	25.78	114	31.11	70.99	11.05	1.62	
	Avg.	55.79	15.63	2.31	11.17	0.09	2.59	2.64	0.93	1.45	0.16	66.57	24.38	115	32.84	71.74	12.25	1.79	
	Min	52.69	14.01	1.50	10.84	0.07	2.35	1.31	0.41	1.21	0.15	58.01	22.62	106	27.37	62.50	9.92	1.54	
	Max	57.17	18.22	3.11	11.44	0.11	2.87	3.64	1.33	1.78	0.18	78.49	25.82	123	37.74	81.22	14.63	2.13	
	Kaveri Shelf																		
	42	76.90	11.81	0.81	4.63	0.04	1.45	0.80	0.86	2.60	0.10	67.48	6.58	39.93	14.47	16.34	23.04	1.52	
	43	83.16	4.24	1.05	3.77	0.05	0.66	1.12	0.55	1.57	0.13	47.71	3.57	13.42	15.78	4.53	4.34	0.85	
	44	83.63	8.05	1.24	3.44	0.05	0.67	1.57	1.47	1.57	0.08	53.56	8.13	42.63	10.38	14.10	77.29	2.19	
	45	45.35	12.18	0.70	8.56	0.02	2.27	8.70	0.75	1.50	0.61	39.47	2.61	15.03	28.74	11.65	3.52	3.65	
	46	49.28	14.66	0.94	13.24	0.03	3.62	3.27	0.57	1.59	1.24	63.01	8.43	171	27.21	32.16	13.30	10.25	
SSK-50	6	51.60	15.90	1.10	9.92	0.01	2.54	1.46	0.59	1.69	0.21	74.42	20.75	160	18.39	30.25	15.69	4.11	
	7	49.60	13.30	0.97	12.83	0.01	3.27	2.61	0.75	1.63	1.13	63.26	16.26	220	16.16	37.22	14.59	13.57	

8	50.30	14.30	0.98	10.97	0.01	3.00	2.82	0.69	1.68	1.05	63.96	18.03	188	18.38	28.74	16.99	11.24
9	56.90	13.00	1.01	8.39	0.01	2.09	2.98	1.11	1.69	0.49	58.85	6.09	37.51	7.54	13.66	8.07	2.59
10	52.30	9.60	0.71	9.77	0.01	3.07	1.84	0.92	1.45	0.29	60.02	5.35	32.68	10.21	12.15	7.35	2.03
11	79.30	6.80	1.01	2.71	0.02	0.73	1.41	1.73	1.34	0.03	49.72	7.14	35.14	7.05		20.70	0.87
12	66.70	13.80	0.67	4.55	0.01	1.30	2.45	2.88	2.14	0.09	54.46	10.24	48.69	9.11	5.38	12.64	1.34
13	62.60	15.40	0.79	5.01	0.01	1.55	2.69	2.95	1.77	0.10	56.93	12.18	103	14.45	19.15	9.26	1.41
14	75.40	8.20	1.14	6.06	0.04	1.58	1.76	1.51	1.28	0.09	53.74	7.07	48.00	10.55	0.62	7.04	0.60
15	61.00	15.90	0.88	6.13	0.02	1.57	2.45	2.50	1.71	0.09	60.42	17.75	134	20.30	41.46	14.50	2.04
16	83.90	5.10	1.63	4.09	0.02	0.88	0.80	0.78	0.83	0.07	58.69	3.91	35.33	5.44	4.78	11.74	1.19
17	88.30	3.10	0.87	3.11	0.01	0.60	0.42	1.95	0.75	0.05	39.14	3.62	17.07	4.75	8.65	4.09	0.58
20	42.80	10.60	0.68	21.91	0.00	5.98	1.64	0.68	1.90	0.57	63.21	10.42	268	19.54	17.98	8.93	3.34
21	53.20	13.20	0.79	10.86	0.01	3.90	2.60	1.50	1.44	0.27	60.10	6.80	73.41	10.70	13.67	6.74	1.93
22	53.50	14.50	0.77	10.37	0.00	2.06	2.09	1.38	1.99	0.23	63.75	9.41	94.65	8.58	65.83	8.43	1.84
23	51.10	17.00	0.94	8.89	0.01	2.23	1.65	0.89	1.73	0.14	72.84	12.07	86.67	10.83	32.66	10.30	2.30
24	77.80	8.70	0.73	3.52	0.01	0.83	1.08	1.32	2.34	0.06	56.71	7.18	36.52	9.05	3.34	18.67	1.58
25	59.90	12.80	0.92	9.13	0.01	2.10	1.36	0.81	2.01	0.25	68.18	8.83	41.59	9.69	15.94	10.70	1.83
26	61.30	13.90	1.10	7.62	0.01	1.98	1.24	0.91	1.92	0.11	70.39	19.02	94.35	18.48	54.36	18.44	2.71
Avg.	63.16	11.50	0.93	7.90	0.02	2.08	2.12	1.25	1.67	0.31	59.17	9.64	84.90	13.57	21.07	14.43	3.15
Min	42.80	3.10	0.67	2.71	0.00	0.60	0.42	0.55	0.75	0.03	39.14	2.61	13.42	4.75	0.62	3.52	0.58
Max	88.30	17.00	1.63	21.91	0.05	5.98	8.70	2.95	2.60	1.24	74.42	20.75	268	28.74	65.83	77.29	13.57

- Major elements determined in salt-free and decarbonated lithogenic fraction
- Trace elements determined in bulk fractions.

Table 5: Rare earth element concentration (ppm) of surface sediments from the eastern continental shelf of India.

Cruise	SPC	La	Ce	Pr	Nd	Sm	Eu	Gd	Tb	Dy	Ho	Er	Tm	Yb	Lu	ΣREE	
		Ganges Brahmaputra Shelf															
SSK 35	1	41	90	8.70	36	6.96	1.32	5.48	0.91	5.09	1.01	2.78	0.41	2.32	0.33	203	
	2	40	87	8.21	35	6.61	1.29	5.40	0.87	4.76	0.96	2.56	0.37	2.09	0.31	194	
	3A	44	93	9.08	37	7.08	1.33	5.13	0.88	4.87	0.96	2.61	0.38	2.06	0.30	209	
	4	53	104	11.02	44	8.34	1.44	5.90	0.99	5.28	1.02	2.68	0.39	2.09	0.30	239	
	5	44	93	9.21	38	7.23	1.33	5.29	0.90	4.99	1.00	2.64	0.39	2.10	0.31	210	
	6	44	95	9.37	38	7.22	1.31	5.09	0.90	4.94	0.98	2.58	0.37	1.99	0.29	212	
	7	37	83	7.41	32	5.75	1.14	4.35	0.75	4.15	0.83	2.26	0.34	1.87	0.28	180	
	8	34	86	6.91	31	5.35	1.06	4.04	0.69	3.83	0.78	2.10	0.32	1.74	0.25	178	
	9	43	90	8.82	36	6.74	1.25	4.89	0.86	4.73	0.94	2.50	0.37	2.03	0.29	203	
	10	58	138	14.52	57	11.01	1.77	7.68	1.34	7.08	1.36	3.51	0.50	2.56	0.37	305	
	11	44	98	8.94	38	6.87	1.24	4.74	0.84	4.67	0.92	2.45	0.36	1.99	0.30	213	
	12	42	92	8.99	37	7.19	1.35	5.06	0.90	4.92	1.01	2.68	0.40	2.16	0.32	205	
	13	42	89	9.11	37	7.33	1.49	5.55	1.06	6.02	1.21	3.18	0.46	2.49	0.36	207	
	14	28	59	5.88	23	4.94	1.08	3.55	0.68	3.98	0.83	2.22	0.32	1.77	0.26	136	
	Avg.	42	93	9.0	37	7.04	1.31	5.15	0.90	4.95	0.99	2.62	0.38	2.09	0.30	207	
	Min	28	59	5.9	23.5	4.94	1.06	3.55	0.68	3.83	0.78	2.10	0.32	1.74	0.25	136	
	Max	58	138	14.5	57.4	11.01	1.77	7.68	1.34	7.08	1.36	3.51	0.50	2.56	0.37	305	
			Mahanadi Shelf														
	15	33	69	6.93	28	5.20	1.05	3.85	0.71	3.98	0.80	2.14	0.32	1.72	0.26	157	
	16	45	105	8.83	39	6.51	1.25	4.80	0.88	5.07	1.06	2.88	0.44	2.46	0.37	223	
	17	53	107	10.72	43	7.95	1.49	5.35	0.97	5.37	1.09	2.95	0.44	2.45	0.36	242	
	18	49	104	10.02	40	7.58	1.43	5.38	1.02	5.65	1.13	3.04	0.46	2.50	0.37	232	
	19	41	97	8.10	35	6.00	1.13	4.09	0.76	4.22	0.86	2.26	0.34	1.88	0.28	203	
20	41	94	8.47	37	6.75	1.37	5.69	0.97	5.49	1.13	3.09	0.47	2.63	0.39	208		
21	48	112	9.71	42	7.41	1.43	6.15	0.97	5.38	1.11	3.08	0.46	2.64	0.40	241		
22	56	144	12.75	55	9.97	1.97	8.59	1.44	8.52	1.79	4.96	0.76	4.28	0.64	310		
23	180	427	41.26	159	29	1.24	20.50	2.64	12.94	2.59	7.51	1.09	6.05	0.92	891		

	24	55	118	11.17	47	8.52	1.56	6.95	1.07	5.87	1.19	3.25	0.48	2.78	0.42	263
	25	51	103	10.61	43	8.28	1.65	6.83	1.14	6.37	1.30	3.59	0.53	3.03	0.45	241
	26	23	54	4.78	20	4.04	0.86	3.68	0.64	3.70	0.77	2.06	0.30	1.64	0.25	119
	27	73	183	19.34	78	13.10	1.61	9.76	1.37	6.85	1.32	3.65	0.53	2.95	0.44	395
	28	50	110	10.60	45	8.46	1.67	7.25	1.25	7.15	1.48	4.01	0.59	3.30	0.49	252
	29	71	171	17.38	72	12.00	1.63	9.19	1.36	7.30	1.50	4.15	0.63	3.50	0.52	374
	30	56	138	13.58	57	10.32	1.62	8.05	1.30	7.53	1.58	4.41	0.67	3.78	0.57	304
	31	62	150	14.51	61	11.00	2.15	8.26	1.22	6.57	1.33	3.67	0.55	3.08	0.46	326
	32	49	117	11.71	48	9.34	1.87	7.76	1.33	7.70	1.59	4.28	0.65	3.59	0.53	265
	33	45	98	8.77	37	6.54	1.34	5.64	0.92	5.20	1.06	2.88	0.42	2.31	0.34	216
	34	41	99	8.75	38	7.16	1.46	6.13	1.03	5.93	1.23	3.41	0.52	2.94	0.44	217
	35	57	128	13.22	53	9.31	1.05	7.54	1.20	6.74	1.45	4.08	0.62	3.54	0.53	287
	Avg.	56	130	12.4	51.2	9.24	1.47	7.21	1.15	6.36	1.30	3.59	0.54	3.00	0.45	284
	Min	23	54	4.78	19.7	4.04	0.86	3.68	0.64	3.70	0.77	2.06	0.30	1.64	0.25	119
	Max	180	427	41	159.0	28.64	2.15	20.50	2.64	12.94	2.59	7.51	1.09	6.05	0.92	892
	Krishna-Godavari Shelf															
	36	35	85	7.42	32	6.38	1.48	5.59	0.97	5.67	1.18	3.23	0.49	2.69	0.40	188
	37	42	90	9.13	38	8.21	2.07	7.12	1.23	7.18	1.51	4.01	0.60	3.30	0.49	215
	38	37	83	8.19	34	7.38	1.82	6.54	1.13	6.59	1.39	3.74	0.56	3.08	0.46	195
	39	25	56	5.93	24	6.05	1.87	5.61	1.00	5.95	1.26	3.34	0.50	2.78	0.41	140
	40	29	68	7.08	30	7.08	2.10	6.49	1.15	6.78	1.44	3.86	0.56	3.16	0.48	167
	41	33	76	7.76	32	7.47	1.98	6.73	1.20	6.93	1.47	3.91	0.58	3.19	0.46	183
	Avg.	34	76	7.58	32	7.09	1.89	6.34	1.11	6.52	1.37	3.68	0.55	3.03	0.45	181
	Min	25	56	5.93	24	6.05	1.48	5.59	0.97	5.67	1.18	3.23	0.49	2.69	0.40	140
	Max	42	90	9.13	38	8.21	2.10	7.12	1.23	7.18	1.51	4.01	0.60	3.30	0.49	215
	Kaveri Shelf															
	42	41	82	8.0	31.9	5.35	1.04	4.26	0.61	3.25	0.68	1.82	0.27	1.50	0.23	183
	43	13	31	3.0	12.1	2.71	0.71	2.27	0.39	2.34	0.51	1.39	0.21	1.18	0.18	72
	44	99	229	23.7	89.8	14.82	1.31	10.67	1.28	5.41	0.95	2.48	0.31	1.77	0.27	481
	45	16	39	3.25	13.8	2.44	0.53	2.16	0.35	2.01	0.42	1.12	0.17	0.85	0.13	82
	46	42	105	9.70	42.3	9.38	2.25	9.13	1.59	9.70	2.07	5.61	0.81	4.43	0.69	245
SSK-	6	35	82	8.13	34	7.34	1.70	6.45	1.19	6.04	1.21	3.53	0.51	3.05	0.49	192

50	7	47	115	10.40	45	9.92	2.45	8.29	1.77	9.85	2.05	5.74	0.78	4.86	0.76	264
	8	46	115	10.91	46	10.75	2.70	8.92	1.91	10.07	2.13	6.06	0.91	5.03	0.87	268
	9	24	52	5.16	23	6.81	2.46	4.97	0.78	3.77	0.75	2.23	0.31	1.86	0.30	128
	10	27	63	5.74	26	4.56	1.04	3.58	0.72	3.69	0.75	2.10	0.29	1.68	0.27	141
	11	40	77	7.67	32	5.02	1.23	4.23	0.68	3.04	0.63	1.87	0.32	1.69	0.32	175
	12	37	81	8.29	36	6.21	1.68	4.89	0.81	3.99	0.77	2.22	0.30	1.84	0.28	185
	13	37	75	7.52	32	5.81	1.84	4.71	0.79	4.01	0.79	2.29	0.32	1.93	0.30	174
	14	27	58	5.52	24	4.02	1.10	3.65	0.59	3.04	0.62	1.82	0.26	1.60	0.26	132
	15	44	93	10.52	44	8.53	2.48	6.82	1.31	6.10	1.29	3.76	0.66	3.30	0.63	226
	16	36	72	7.24	31	4.98	0.94	4.14	0.66	3.08	0.60	1.68	0.23	1.31	0.21	164
	17	14	27	3.14	14	3.25	1.02	1.91	0.37	1.92	0.40	1.15	0.17	1.02	0.17	69
	20	28	71	6.84	31	6.17	1.59	5.21	0.96	5.04	1.02	2.92	0.39	2.38	0.36	163
	21	27	60	6.08	27	4.72	1.15	3.55	0.66	3.36	0.67	1.89	0.26	1.59	0.24	139
	22	27	57	5.95	26	4.73	1.26	4.31	0.72	3.69	0.74	2.15	0.29	1.80	0.28	136
	23	28	62	6.47	28	5.02	1.24	3.86	0.75	3.90	0.78	2.26	0.32	1.93	0.31	145
	24	35	76	7.60	33	5.54	1.18	4.31	0.71	3.46	0.67	1.92	0.26	1.59	0.25	172
	25	30	72	6.87	32	5.42	1.21	4.35	0.80	4.19	0.82	2.32	0.31	1.92	0.29	162
	26	40	94	9.59	41	7.59	1.69	6.35	1.12	5.73	1.13	3.32	0.45	2.86	0.43	215
	Avg.	35	79	7.80	33	6.30	1.49	5.12	0.90	4.61	0.93	2.65	0.38	2.21	0.35	180
	Min	13.4	27	2.98	12.1	2.44	0.53	1.91	0.35	1.92	0.40	1.12	0.17	0.85	0.13	65
Max	99	229	23.7	90	14.82	2.70	10.67	1.91	10.07	2.13	6.06	0.91	5.03	0.87	497	

- REEs determined in bulk fraction

Table 6: A-priori compositions for the elements of the five sources

Element/source	Ganga	Mahanadi	Godavari	Krishna	Kaveri
Al (%)	8.78	7.21	8.47	7.71	1.63
Ti (%)	0.50	0.51	1.20	1.60	0.52
Fe (%)	4.18	3.65	7.61	7.87	2.17
Mg (%)	1.33	0.90	1.45	1.70	0.36

Figure captions

Fig. 1: Simplified geological map of South Asia including India, Nepal, Bhutan, Bangladesh, and Myanmar modified after U.S. Geological Survey Open-File Report 97-470-C (For a more detailed map, refer Wandrey and Law, (1998) or visit the site <https://pubs.er.usgs.gov/publication/ofr97470C>). The color codes shown in the legend represent the age of the lithological formations which include igneous, metamorphic, sedimentary, extrusive, and undivided rocks. Smaller geological units within the Paleozoic, Mesozoic, and Cenozoic eras were combined to simplify the map. The Deccan Traps which fall within the Mesozoic – Cenozoic boundary are marked in a different color legend as it is a major lithological type through which two major peninsular Indian rivers drain. Major lithological units (HHCS- Higher Himalayan crystalline series, LH – Lesser Himalayas, TSS -Tethyan Sedimentary series, TTGs - tonalite-trondjemite gneisses, RSR- recent sedimentary rocks, SGT- Southern granulite terrain) and rivers are marked in the map. Sampling locations of sediments studied here are marked with ‘star’ symbols. Black circles mark the major cities while the solid and dotted arrows indicate the East India coastal current (EICC) during winter (NE) and summer (SW) monsoon respectively.

Fig. 2: Distribution of sand, silt, and clay content (%) in the eastern continental shelf sediments of India.

Fig. 3: Distribution of major clay mineral content (%) in the eastern continental shelf sediments of India.

Fig. 4: Map showing the spatial distribution of some diagnostic major elements in lithogenic fraction along the eastern continental shelf of India. CaO is of non-carbonate fraction.

Fig. 5: Spatial distribution of Total REE, Eu anomaly, Th/U ratio and chemical index of alteration (CIA) in sediments from the Eastern continental shelf of India (Data presented on the carbonate free basis).

Fig. 6: Shale-normalized REE patterns of the sediments from the eastern continental shelf of India (REE values are calculated on carbonate free basis) plotted along with probable sources for sediments to the east coast rivers (Biotite Leucogranite, Tourmaline Leucogranite along with HHCS: Ayres and Haris, 1997; TTG and Closepet granites: Martin and Moyen, 2005; Charnokites: Stähle et al., 1987; Gneisses: Mahabaleshwar et al., 1995; mafic granulites and felsic granulites: Rajamani et al., 2009; Ganga river sediments, suspended sediments; Singh 2010; Loess: Taylor et al., 1983).

Fig. 7: Scatter plots of TiO₂ content versus sand (a), silt (b), and clay content (c); Al₂O₃/ SiO₂ versus sand (d), silt (e), and clay content (f); Na₂O/K₂O versus Al₂O₃/SiO₂ (g) and total REE versus Al₂O₃/SiO₂ (h). All data are presented on a carbonate free basis after eliminating samples with less than 20% clay content to remove the influence of sorting.

Fig. 8: Plot of all the sediments (on a carbonate free basis) from the eastern continental shelf of India in the A–CN–K diagram. For comparison are also plotted charnokites (Condie and Allen, 1984, Janardhan et al., 1983), Gneisses (Mahabaleshwar et al., 1995), Deccan Basalt (Ghose, 1976), THB, HHCS, LH and Siwalikh (Galy and France-Lanord., 2001), Granites (Sharma and Rajamani, 2000), Upper Continental Crust (UCC) and Post Archean Australian Shale (PAAS) (Taylor and McLennan, 1985). Note that all the G-B shelf sediments plot between the fields of HHCS, and LH rocks indicating that these rocks have acted as source rocks, while the Mahanadi shelf sediments plot much above the HHCS field and fall within the LH compositional field suggesting a much-weathered source such as LH to the sediments. The Kaveri and K-G shelf sediments plot along the A-CN trend line and parallel to the G-B and Mahanadi shelf sediments. The southern shelf sediments plot between the compositional fields of basalts, charnokites, and granites suggesting a mixed nature for these sediments.

Fig. 9: Sampling stations selected as end members for modeling the dispersal of coastal sediments offshore. The station closest to the coast (★) was taken to represent the source composition of hinterland source rocks in the respective drainage basins.

Fig. 10: Source and compositional discrimination plot of (a) Sc versus Th (fields after Mir et al., 2022); (b) Th/Sc versus Cr/Th (fields after Luo et al., 2021); (c) Ni versus TiO₂ (fields after Zhang et al., 2020); and (d) Co/Th versus La/Sc diagram (fields after Zhang et al., 2020). The trace element data used here are calculated on a carbonate free basis.

Fig. 11: Ternary plot of La-Th-Sc for source rock determination. Note that all samples plot in between the fields of average granite, granodiorite, and basalt. The G-B, Mahanadi and Kaveri shelf sediments indicate a mixed signature of a mafic contribution probably from the Deccan basalts and felsic contribution from the HHCS metasediments, peninsular granitic and gneissic complex from south India. The K-G shelf sediments however receive a greater proportion of sediments from a basic end member probably the Deccan Traps.

Fig. 12: Map showing the geographical extent of the provenance and the possible natural sediment dispersal pathways in the continental margin sediments of India inferred from least square minimization of geochemical data. A schematic representation of the surface currents in the margins is also shown. The solid lines represent the current directions during the summer monsoon while the dashed lines represent the winter monsoon directions.

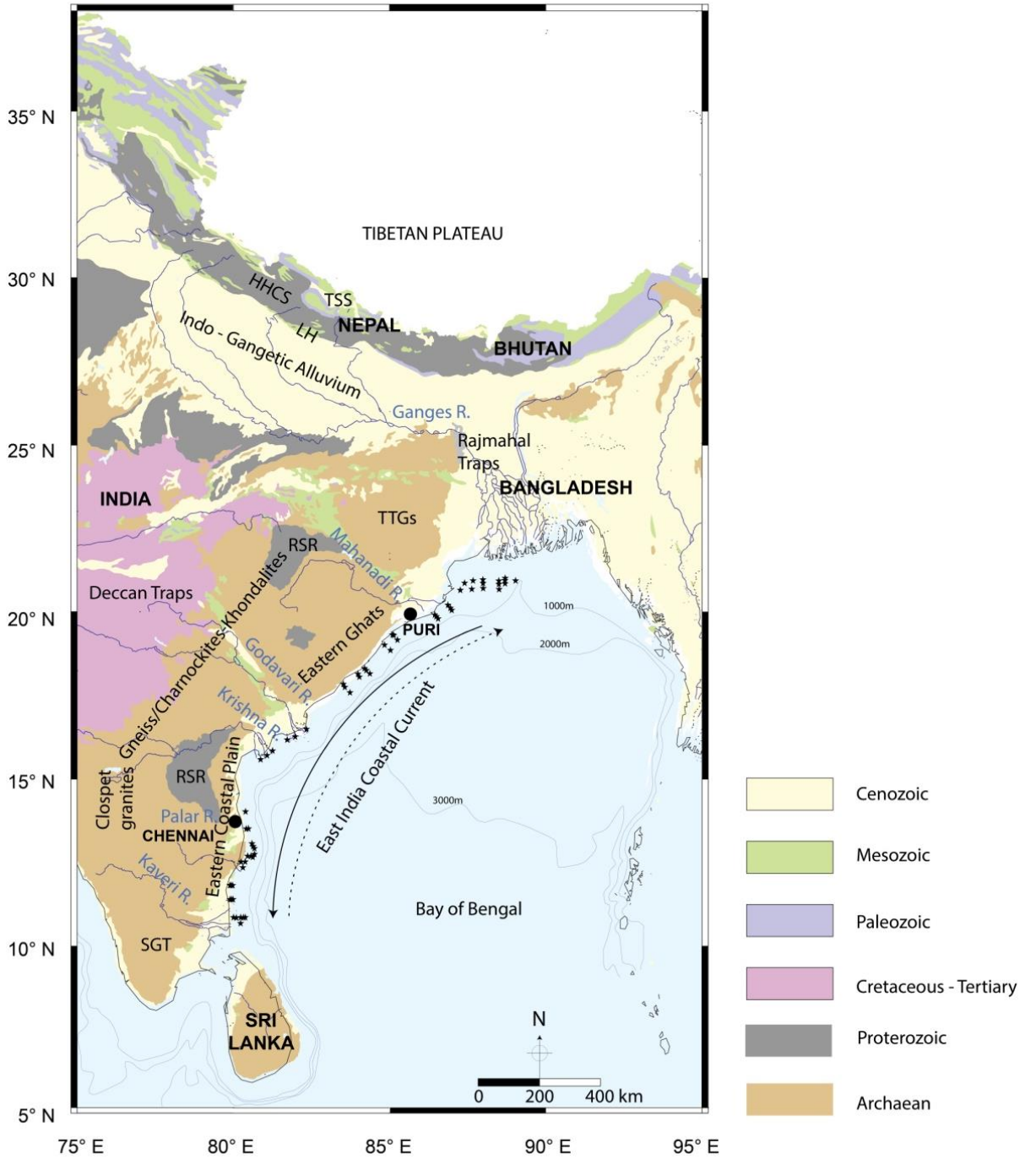


Fig. 1

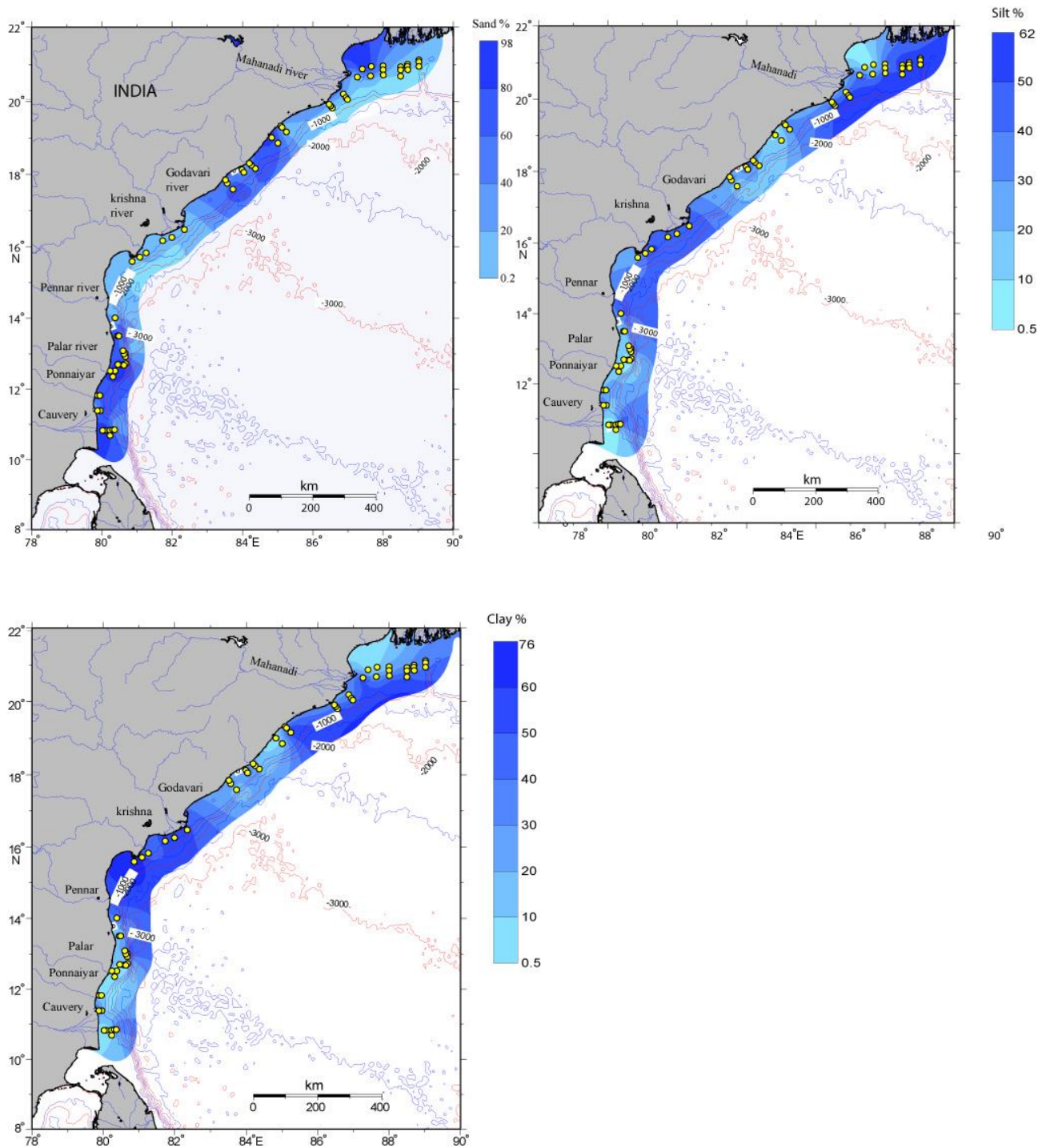


Fig. 2

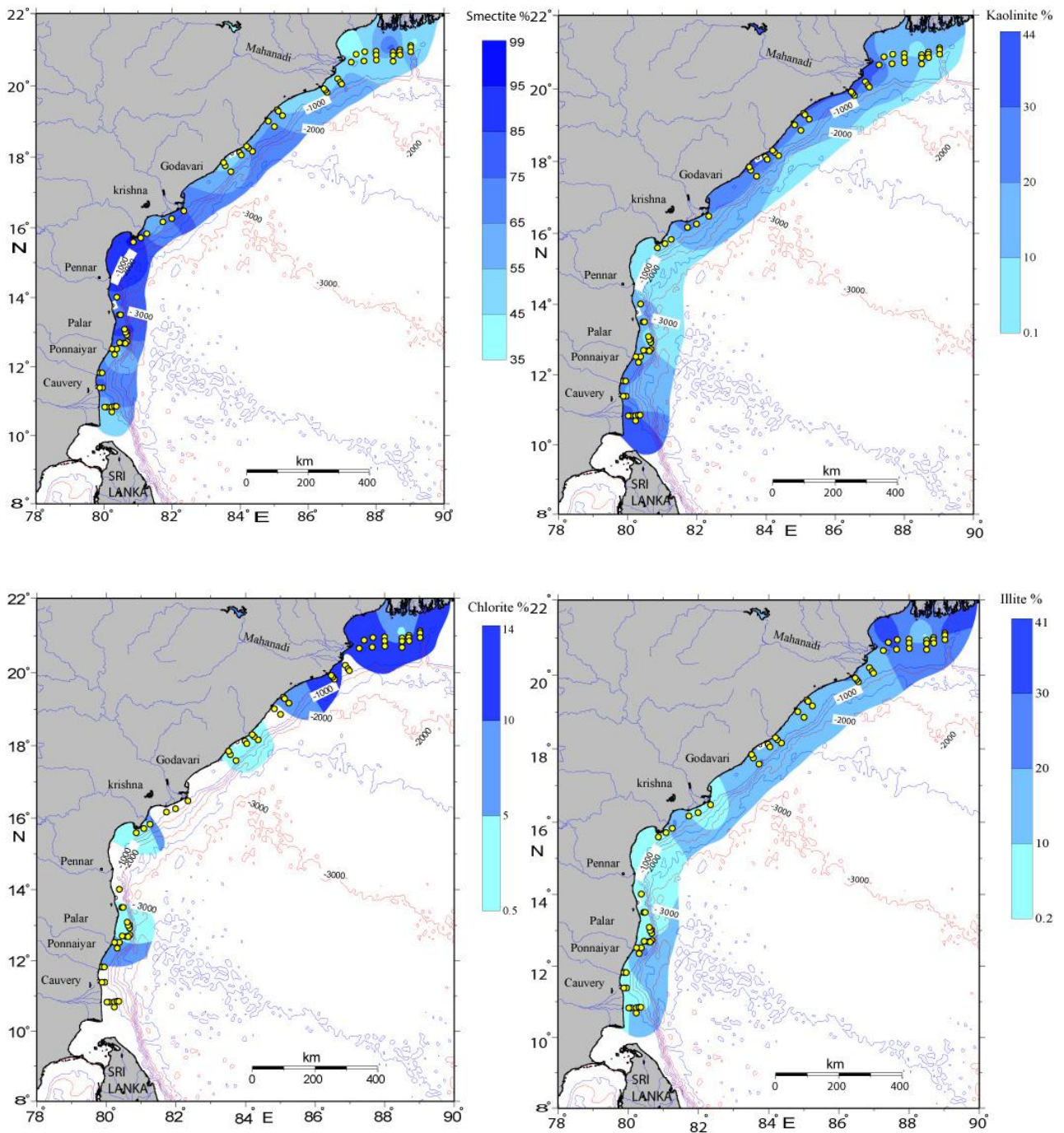
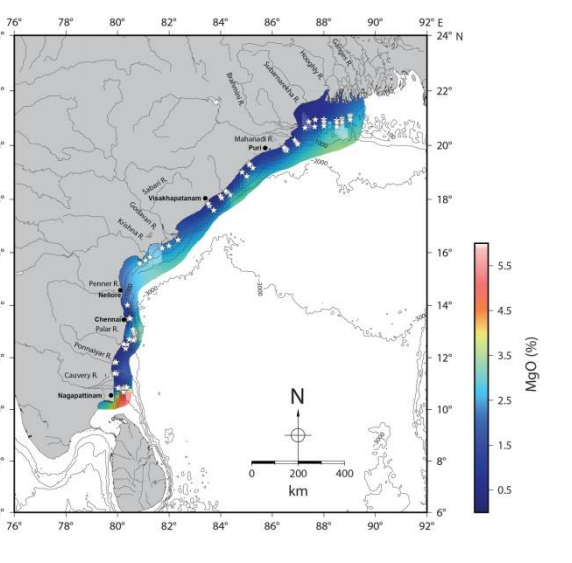
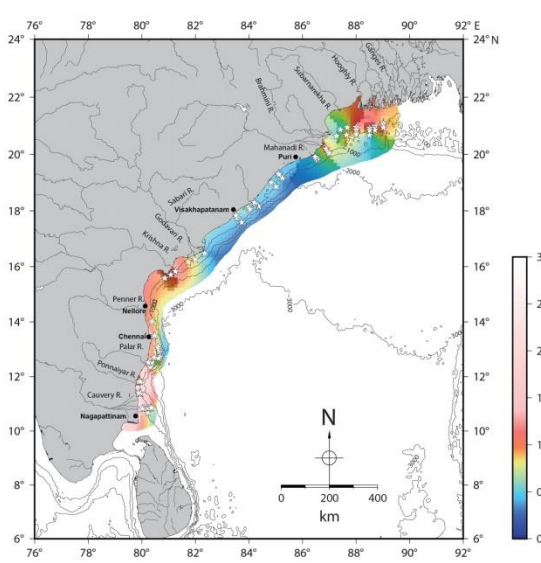
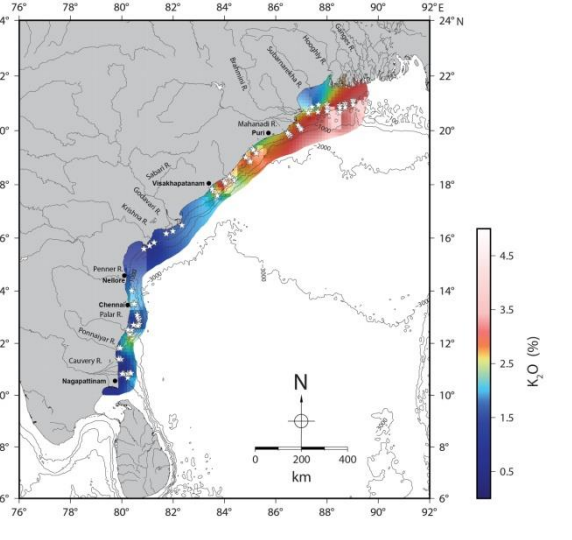
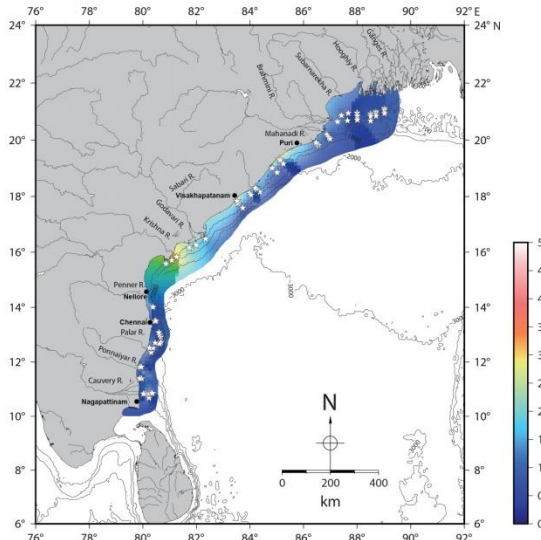
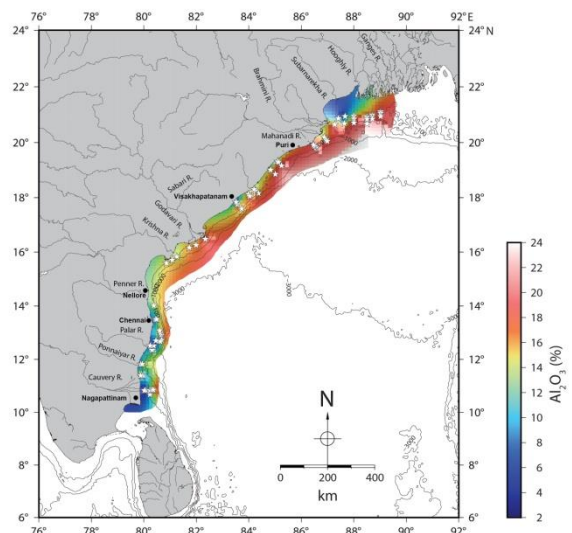
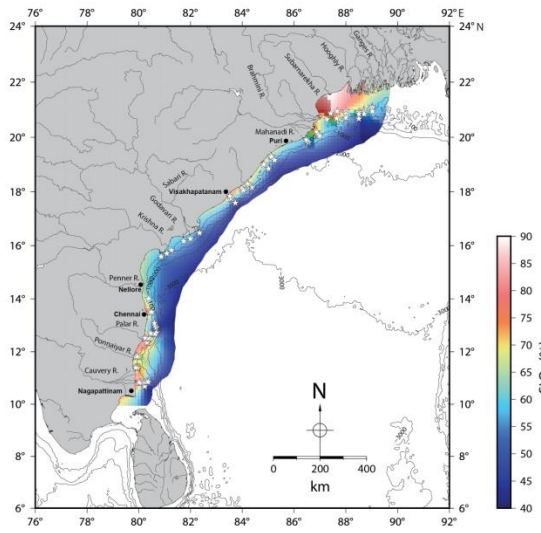


Fig. 3



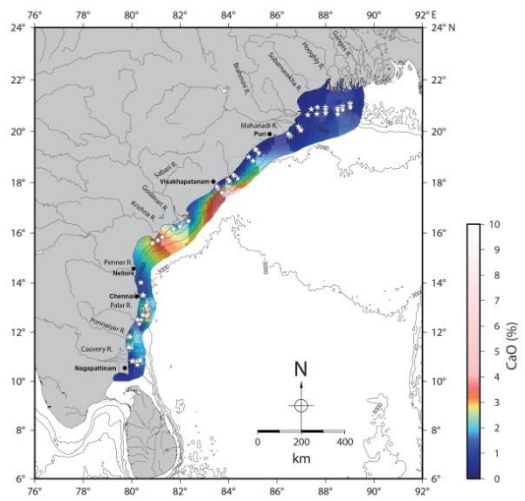


Fig 4

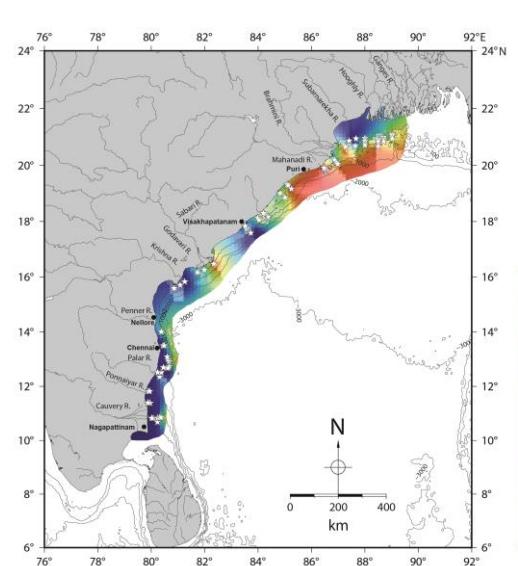
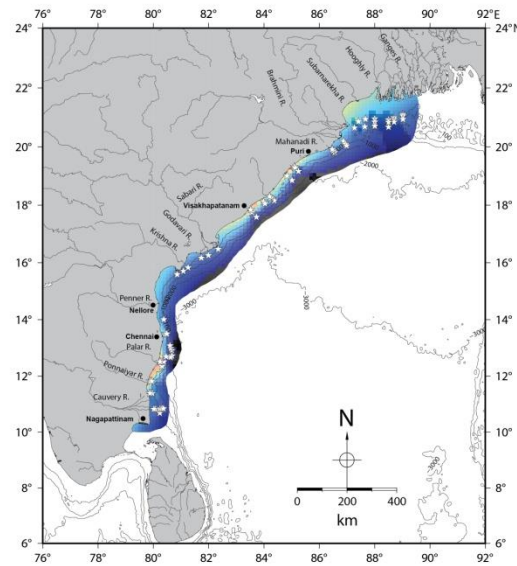
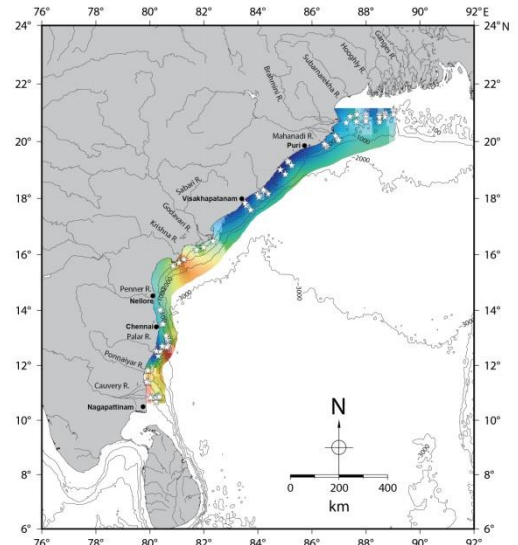
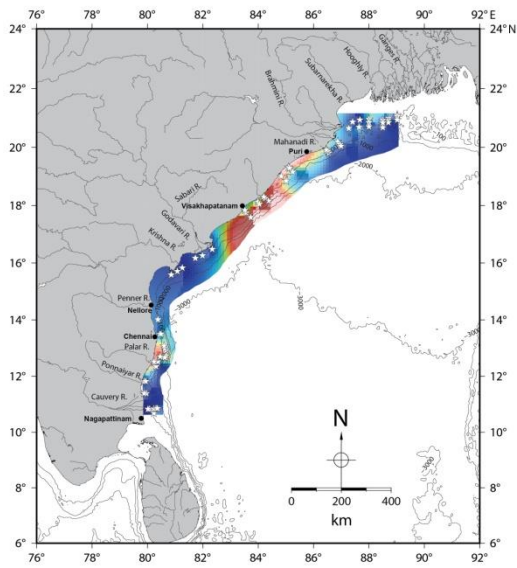


Fig. 5.

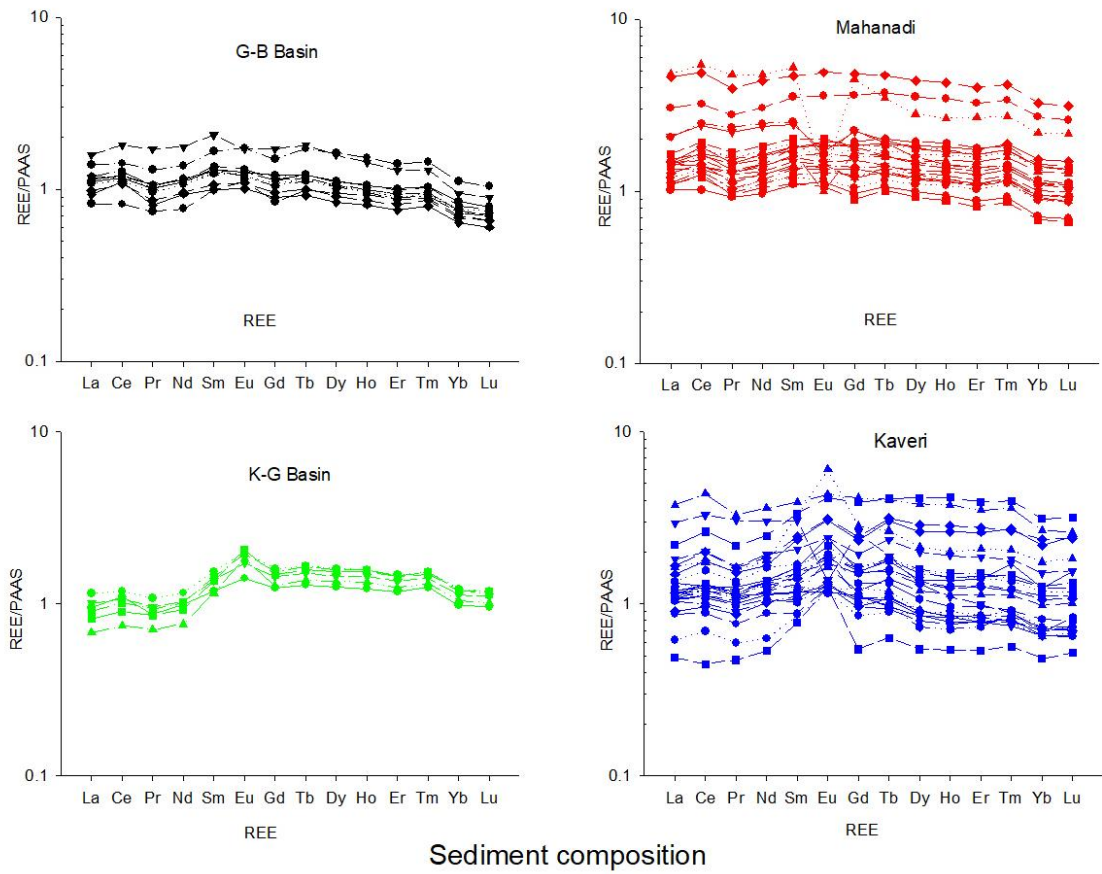
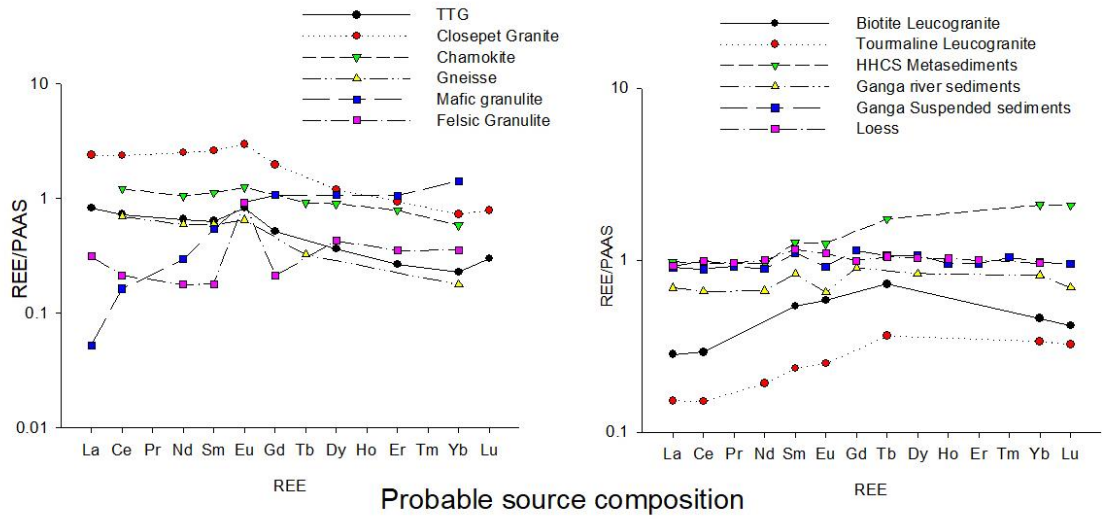


Fig. 6

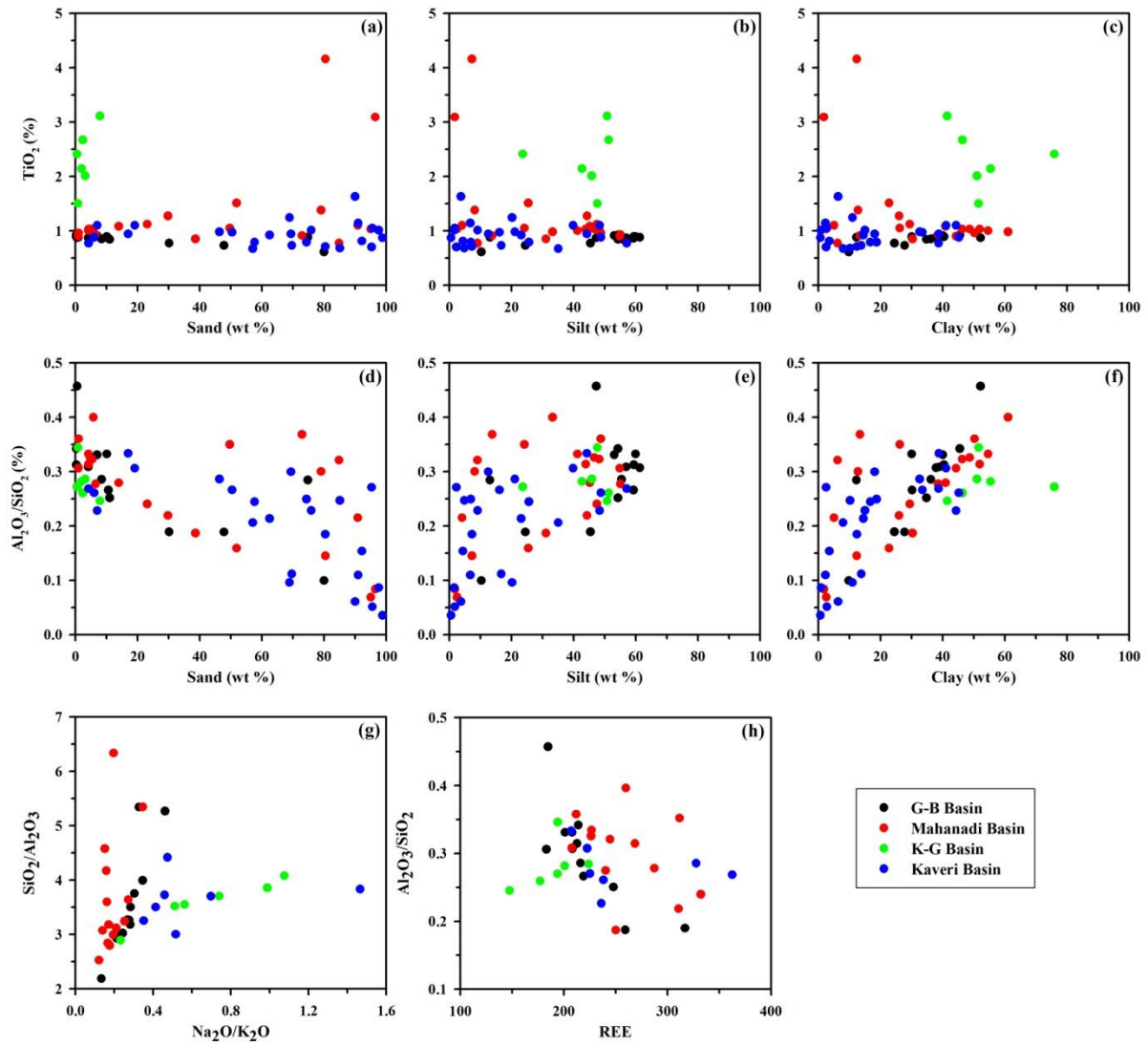


Fig. 7.

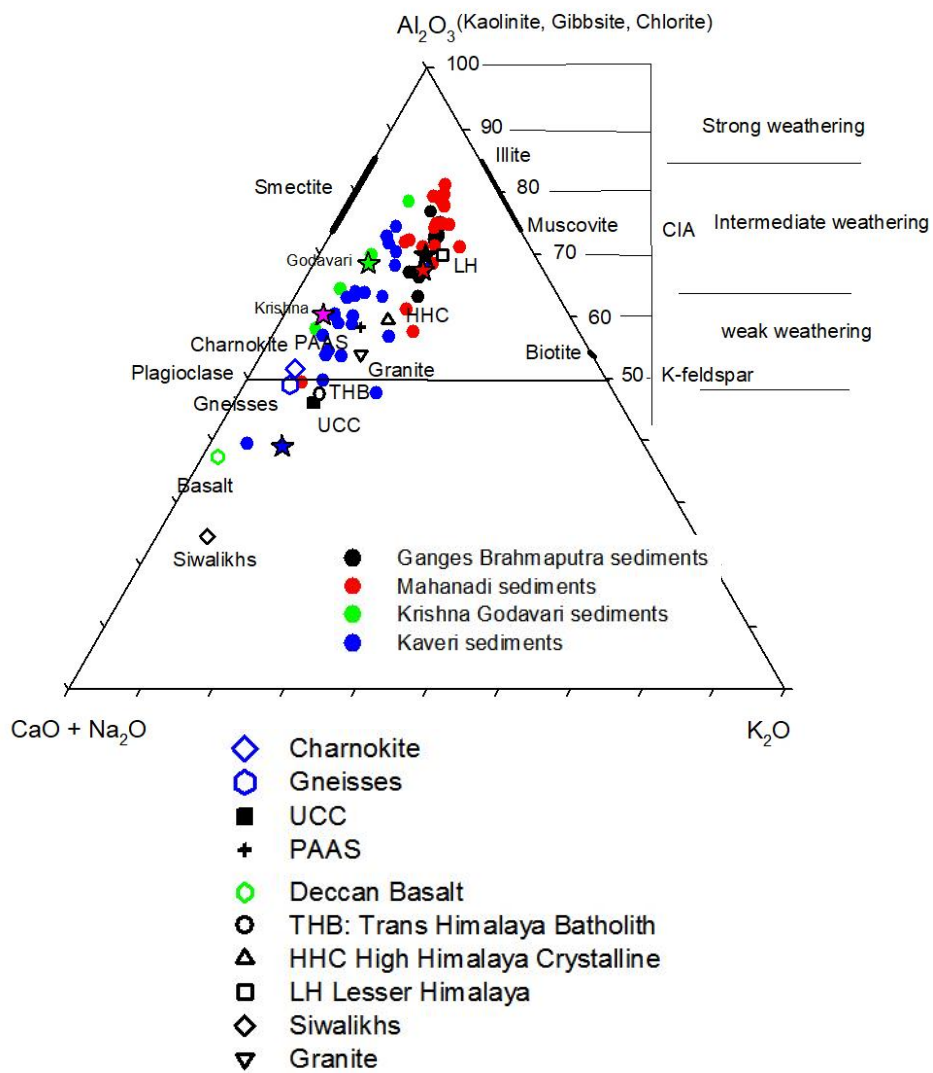


Fig. 8

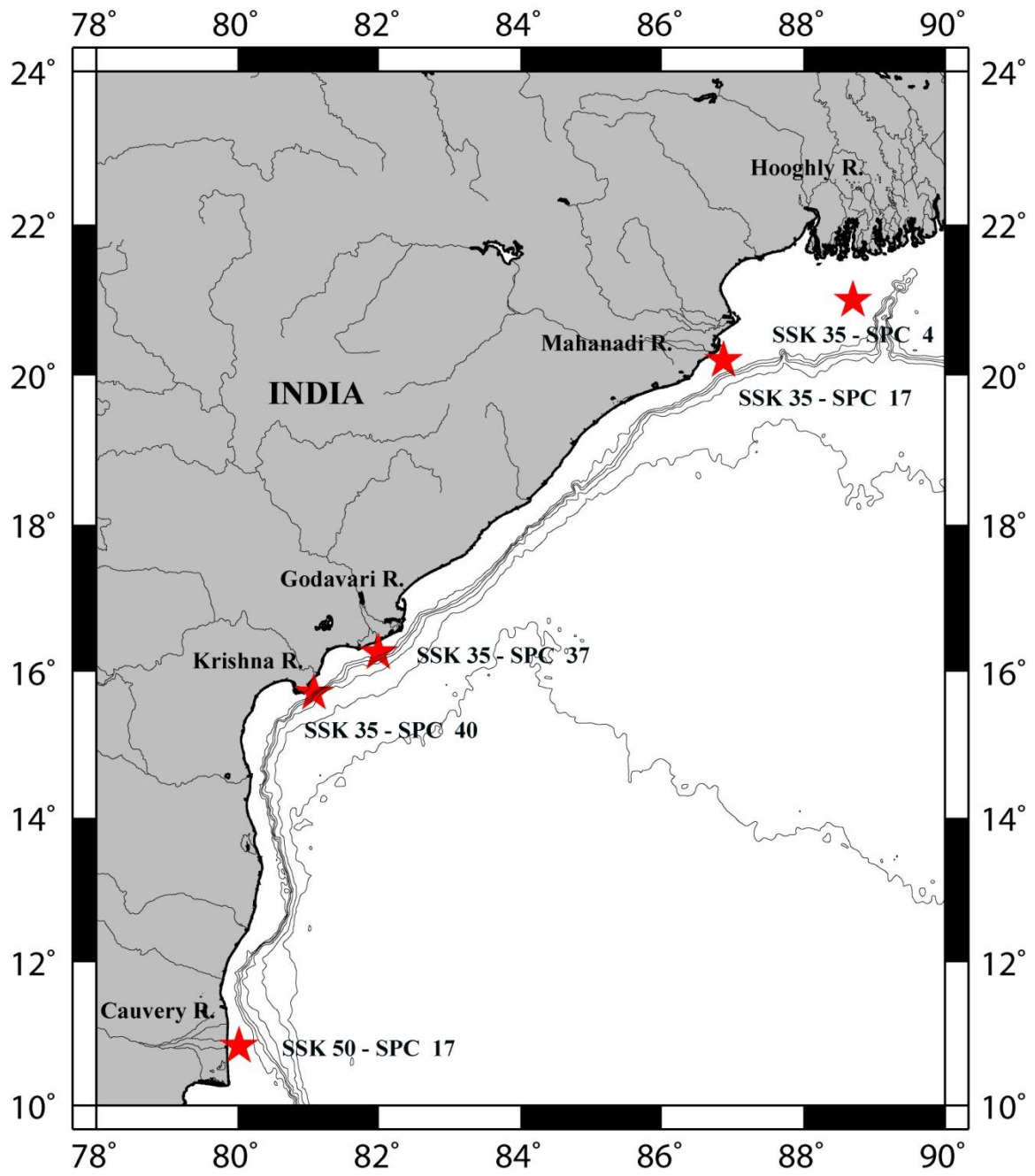


Fig.9

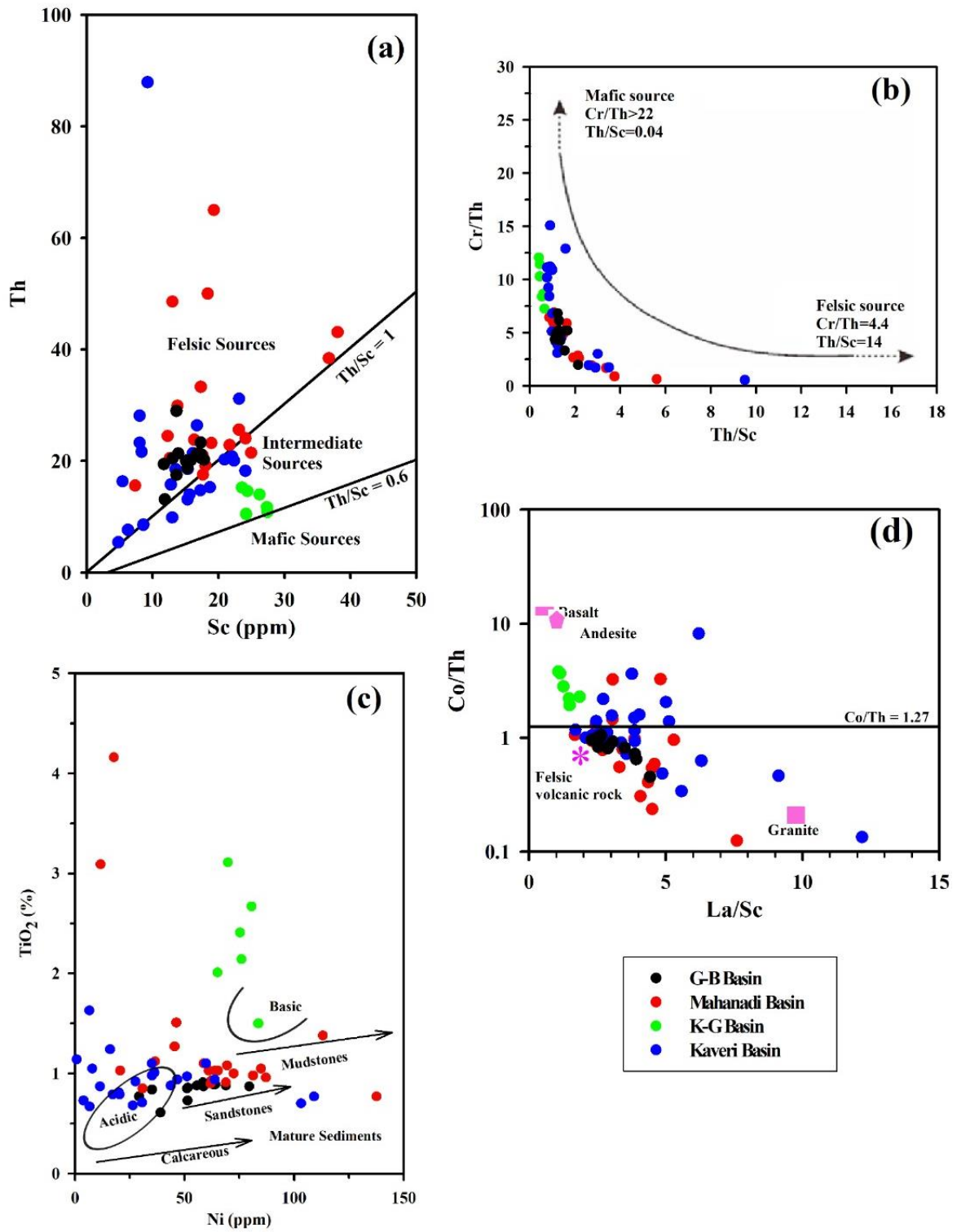


Fig. 10

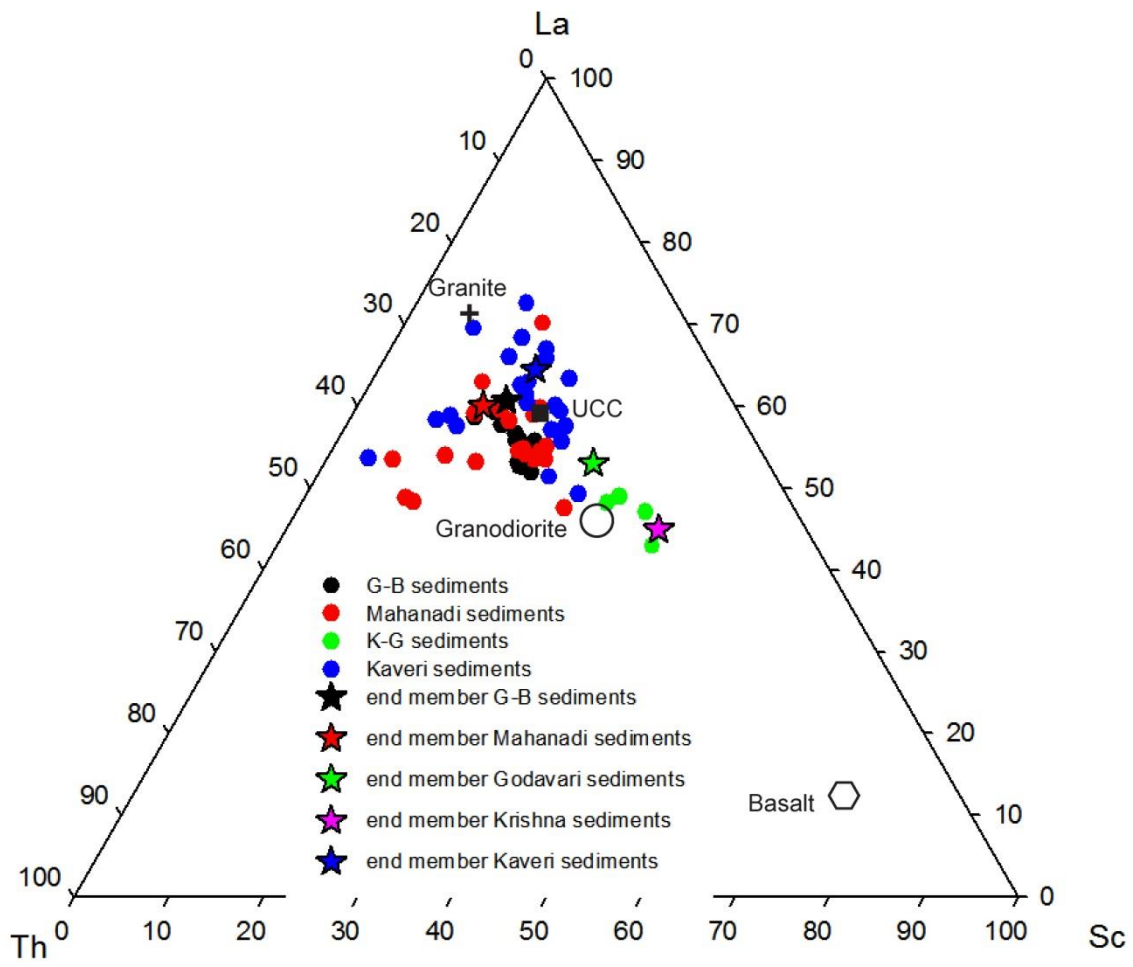


Fig. 11

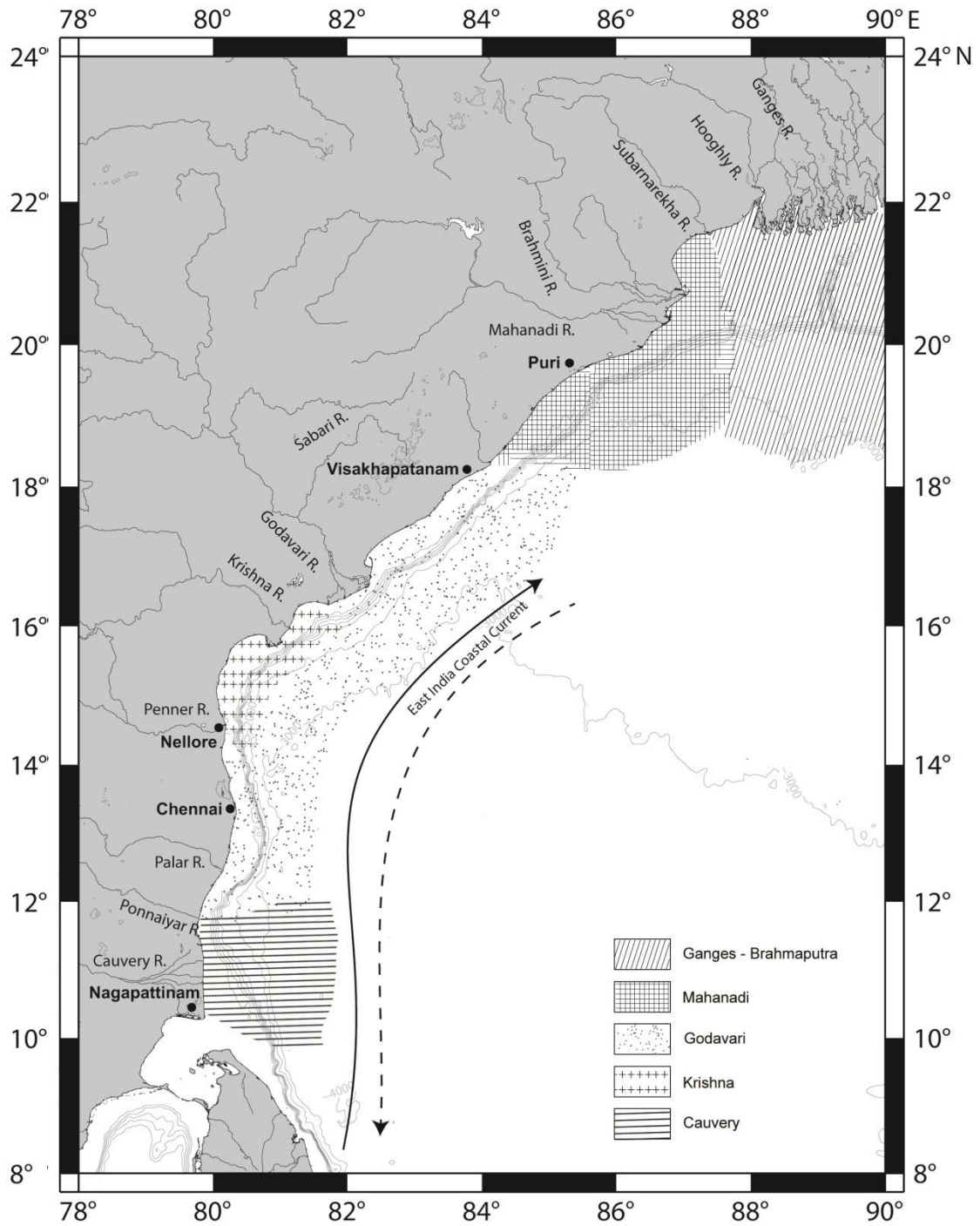


Fig. 12